Missouri S&T Library and Learning Resources

Scholars' Mine

Masters Theses

Student Theses and Dissertations

1966

A nonlinear sampled data feedback control system employing pulsed thrust position control

John D. Corrigan

Follow this and additional works at: https://scholarsmine.mst.edu/masters_theses

 Part of the Electrical and Computer Engineering Commons

Department:

Recommended Citation

Corrigan, John D., "A nonlinear sampled data feedback control system employing pulsed thrust position control" (1966). *Masters Theses*. 5764.
https://scholarsmine.mst.edu/masters_theses/5764

This thesis is brought to you by Scholars' Mine, a service of the Missouri S&T Library and Learning Resources. This work is protected by U. S. Copyright Law. Unauthorized use including reproduction for redistribution requires the permission of the copyright holder. For more information, please contact scholarsmine@mst.edu.

A NONLINEAR SAMPLED DATA FEEDBACK CONTROL SYSTEM EMPLOYING PULSED THRUST POSITION CONTROL

BY

JOHN D. CORRIGAN

A

THESIS

submitted to the faculty of

THE UNIVERSITY OF MISSOURI AT ROLLA

in partial fulfillment of the requirements for the

Degree of

MASTER OF SCIENCE IN ELECTRICAL ENGINEERING

Rolla, Missouri

1966

Approved by

T Mack (advisor) H A Brown

Robert D Chenowith S J Pagano

ABSTRACT

This thesis shows that reaction jet thrust pulses, each of constant amplitude and time duration, in conjunction with sampled data error information can provide satisfactory position and/or attitude control for space vehicles.

Incremental phase-plane analysis of the system yields a technique for determining system response and suggests a means of compensation. Control system response for the vehicle under the influence of external forces is shown to be satisfactory by digital computer simulation.

ACKNOWLEDGEMENTS

The author of this thesis wishes to express his appreciation to Dr. T. L. Noack for his suggestions and guidance during the course of this research.

He also wishes to thank Dr. R. D. Chenoweth for his encouragement and the use of important reference material.

He is also grateful for the use of the Computer Center's facilities.

Finally, the author wishes to thank his wife for her patience in the typing of this manuscript.

TABLE OF CONTENTS

LIST OF SYMBOLS

Symbol	Definition
A	slope of ramp input signal
α	error dead zone limit
b, B*	compensation signal
c, C	Total output position
c', C'	total output position rate
c_{ok}, C_{ok}	output position due to kth control pulse
c_1, C_1	output position due to the external force
c'_1, C'_1	output position rate due to the external force
Δ	change in value; forward difference
e, E	error signal (or base of natural logarithms)
e*, E*	sampled error signal
e_1, E_1	cascade compensator error signal
e_2, E_2	feedback signal for K≠1
e_3, E_3	error signal for K≠1
F	control force amplitude
F_1	magnitude of constant external force
f_o	control force
f_{ok}, F_{ok}	kth control force pulse
f^*_{ok}, F^*_{ok}	sampled control force
G	vehicle transfer function
K	compensator gain
K_f	gain multiplication factor
K_2	trajectory slope
K_3	constant of proportionality

kT	kth sample instant
L	Laplace transform operator
M	mass of vehicle
N	functional notation for nonlinearity
r,R	input signal (commanded position)
s	Laplace transform variable
t	time
T	sampling period
T_p	control force duration
T_d	control force application delay time
u	unit step
x, X	dummy variable
y, Y	dummy variable
Z	"Z" transform operator
z	"z" transform variable

* When both small and capital letters appear, the small letter denotes a function of time and the capital letter denotes the transformed variable.

LIST OF FIGURES

CHAPTER I

INTRODUCTION

Recent years have found an increased interest in space exploration and utilization. Space vehicles with many types of attitude and position control systems have been designed. Common to many of these vehicles is the use of small thrust rockets to impart a directional force or an attitude control torque. These systems usually employ elaborate methods to control the amplitude, duration, or time of application of the rocket thrusts.

Orbiting space laboratories and other manned space vehicles are projects of the near future. With projects of this type comes the need to have simply equipped supply vehicles rendezvous with the manned vehicle. One type of control system which could be used for either position or attitude control on such a supply vehicle would employ small thrust rockets that were all programmed to have equal thrust amplitudes and time durations. The fixed values of these parameters would allow the design of a simpler control system than those ordinarily employed.

The control system would operate in the following manner. Position error information would be gathered by a radar or some other type of error sensing device and would be in sampled data form. If the position error exceeded some set threshold value at the sampling instant, a correction thrust pulse would be commanded to reduce the recorded error.

If the position error was less than the threshold value at the sampling instant, no thrust pulse would be commanded.

The control system described above amounts to a sampled data feedback system having a nonlinearity in its forward path. It is this nonlinearity and the inclusion of external forces which may act on the vehicle that cause difficulty in analysis of the control system.

This thesis examines the characteristics of the nonlinear sampled data feedback control system described above. Since the general characteristics of this system are of interest, a single axis translational position control system is used as a model. This model was chosen since, for a three axis system, the equations for translational motion are independent while the equations for rotational motion are coupled.

Often, the only method available to analyze a nonlinear sampled data control system is the simulation of the specific system using analog, digital, or hybrid computing techniques. Therefore, of secondary interest in this thesis is the application of incremental phase-plane analysis to study the system's general characteristics.

CHAPTER II

REVIEW OF LITERATURE

Research into space utilization and vehicle design began in earnest during the 1950's. During the later portion of this decade, plans began to be made to orbit satellites and later to have manned space flight. Inherent in these plans were attitude control design problems. Several investigators have reported on the use of reaction jets or rockets for spacecraft attitude stabilization.

In April 1959, Pistiner (1) developed certain non-linear analysis and synthesis techniques as applied to on-off attitude control systems. The author used phase-plane analysis to study a hydrogen peroxide reaction jet control system. He established the requirement for lead compensation networks to achieve stable limit cycle operation and discussed the effect of time delays on system performance. Fuel consumption was shown to be dependent on lead network configuration and a synthesis method for optimization of the compensation networks to achieve minimum fuel consumption was applied to this continuous feedback control problem.

Marx (2), in February, 1961, discussed various design aspects of attitude control systems as required by the different phases of manned orbital flight. These phases were: boost, orbit injection, orbit, orbit ejection, re-entry, and landing. The applicability of numerous figures of merit to the attitude control problems during the different

phases of flight were studied. Several appropriate and usable continuous feedback control systems were offered as possible solutions.

During 1962, research in the area of reaction jet attitude control systems increased. In April, a report was published by Dahl (3) which considered the effects of external torques on the limit cycle operation of a reaction jet attitude control system. Expressions were developed for the impulse requirements of the limit cycle operation of a system under the action of external torques. Phase-plane analysis was used to study the system response for combinations of thrust pulse width modulation and pulse frequency modulation. Among the results obtained was the fact that destabilizing torques can be used to reduce the impulse requirements below those of a torque free system.

Also during April, 1962, Gaylord (4) described the development of a new approach to pulsed jet attitude control which makes use of logical control to design efficient limit cycle operation. He also showed that by proper logical switching of the gas reaction thrusts one can eliminate the use of rate measuring and damping networks. He also describes the use of controlled pulse lengths to reduce the effect of turn-off delays in order to minimize limit cycle amplitude and fuel consumption.

In October, 1962, Vaeth (5) described a reaction jet control technique which combines low-thrust vapor jets and time-dependent on-off switching circuits. Analog computer

studies of the system were made to determine the capabilities and limitations of this approach. The paper also presents design guides for synthesizing the system to meet particular sets of performance specifications.

Vaeth (6) at a later date, January, 1965, expanded his earlier paper in order to compare three different impulse modulation techniques. Analog computers were used to simulate the reaction control systems. Based on these analog results and theoretical correlation, design guides were evolved for selecting control system parameters and minimizing fuel consumption.

All of the attitude control systems referenced above had two basic common characteristics: 1. Each utilized continuous information feedback in making control corrections, 2. Each utilized a reaction thrust as the control element. None of the reports examined considered the use of sampled data information to make control decisions, but each yielded an insight into the operation of reaction jet control systems.

CHAPTER III

MATHEMATICAL MODEL

A general description of the control system examined in this thesis is given in Chapter I. It is the intent of this chapter to state more precisely the physical characteristics of the control system. A mathematical model is derived from this statement of the system. It is this model upon which the analysis of the following chapters is based.

For the vehicle to rendezvous with another vehicle or to be at a particular position in space at any given instant of time, its position must be closely controlled. If the speed in the forward direction is constant (coasting), then the vertical and horizontal positions must be controlled as a function of time. It is the position control in one of these directions that is investigated in this thesis.

The object under control is a mass which is assumed to remain constant. This mass is accelerated by pulsed control thrusts and external forces. The control thrusts, as described previously, are all of equal amplitude and duration. They are commanded when error between the actual position and the input signal (commanded position) exceeds a preset limit and they are directed so as to decrease the error being sensed.

The external forces mentioned would include those due to gravitational gradient, Coriolis acceleration, solar wind, magnetic fields, and so forth.

The error signal which commands the control thrusts is assumed to be in sampled form. This would be the case, for instance, if a scanning radar were used to sense position error between two space vehicles.

The system can be represented as shown by the block diagram in Figure 1. The output of the nonlinearity may be described by

$$f_o(t) = \sum_{k=0}^{k=\infty} N(e(kT))[u(t-kT-T_d) - u(t-kT-T_d-T_p)] \quad (3\text{-}1)$$

and

$$N(e(kT)) = \begin{cases} F & , e(kT) \geq \alpha \\ 0 & , |e(kT)| < \alpha \\ -F & , e(kT) \leq -\alpha \end{cases} \quad (3\text{-}2)$$

where kT = sampling instant
T_d = control force application delay time
T_p = control force duration
F = control force amplitude
α = error dead zone limit.

If the delay time, T_d, is small compared to the sampling period, it can be neglected. This can be shown by consideration of the effect the time delay would have on the system response. For purposes of analysis, the time delay, T_d, will be neglected. Equation 3-1 then becomes

$$f_{ok}(t) = N(e(kT))[u(t-kT) - u(t-kT-T_p)] \quad (3\text{-}3)$$

where k denotes the kth term of the summation given in equation 3-1. The Laplace transform of equation 3-3 yields

$$F_{ok}(s) = N(e(kT))\left[\frac{(1-e^{-T_p s})}{s} e^{-kTs}\right]. \quad (3\text{-}4)$$

Following the example of reference (7) and expressing $e^{-T_p s}$ as an infinite series, equation 3-4 becomes

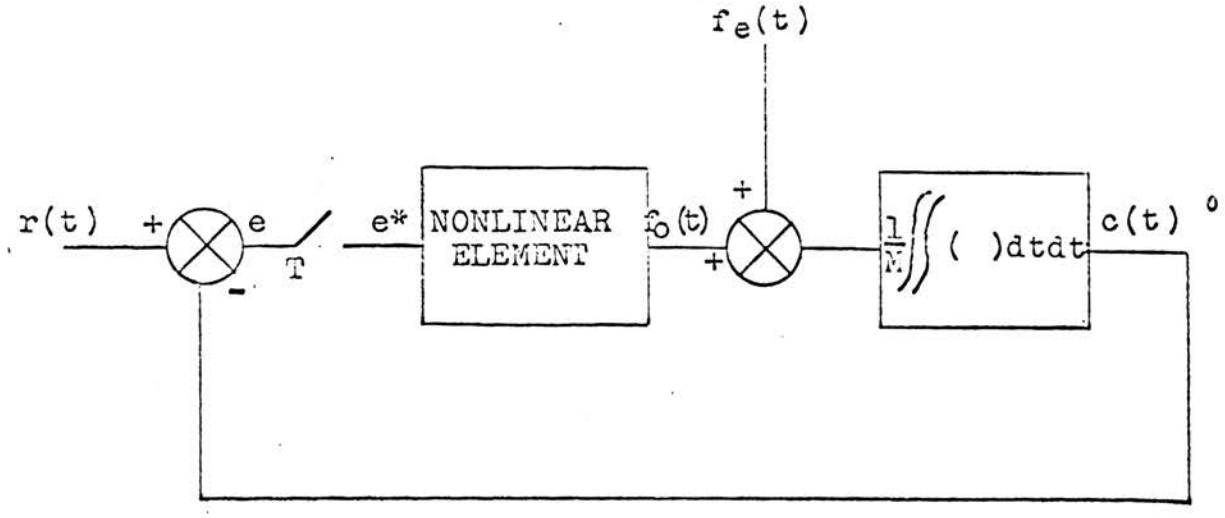

Figure 1. Block Diagram of Position Control System

The symbols used are defined as follows:

$c(t)$ = output position
$r(t)$ = input signal (commanded position)
$e(t)$ = error signal
$e^*(t)$ = sampled error signal
$f_o(t)$ = control force
$f_e(t)$ = external force
M = mass of vehicle
T = sampling period

$$F_{ok}(s) = N(e(kT))\left[\frac{e^{-kTs}}{s}\left(1-\left(1-T_p s+\frac{(T_p s)^2}{2!}-\frac{(T_p s)^3}{3!}+\ldots\right)\right)\right]$$

$$= N(e(kT))T_p\left[1-\frac{T_p s}{2!} + \frac{T_p^2 s^2}{3!}\ldots\right]e^{-kTs}. \qquad (3\text{-}5)$$

If $f_e(t)$ and all initial conditions are neglected, the transfer function $G(s) = C_{ok}(s)/F_{ok}(s)$ can be written as

$$G(s) = \frac{C_{ok}(s)}{F_{ok}(s)} = \frac{1}{Ms^2} . \qquad (3\text{-}6)$$

Therefore,

$$C_{ok}(s) = \frac{N(e(kT))T_p}{M}\left[\frac{1}{s^2} - \frac{T_p}{2!s} + \frac{T_p^2}{3!} -\ldots\right]e^{-kTs}. \qquad (3\text{-}7)$$

Since, from consideration of the physical system an impulsive response cannot exist,

$$c_{ok}(t) = \frac{N(e(kT))T_p}{M}\left[(t-kT) - \frac{T_p}{2}\right]u(t-kT). \qquad (3\text{-}8)$$

The change in position during the period between error samples, i.e. between $t=kT$ and $t=kT+T$, due to an error at $t=kT$ is given by $\Delta c_{ok}(kT)$ where

$$\Delta c_{ok}(kT) = \lim_{t \to (kT+T)^-} c_{ok}(t)$$

$$= \frac{N(e(kT))T_p}{M}\left[T-\frac{T_p}{2}\right]$$

$$= \frac{N(e(kT))T_p}{M}\left[1-\frac{T_p}{2T}\right]T. \qquad (3\text{-}9)$$

If the gain multiplication factor is defined as

$$K_f = T_p\left[1-\frac{T_p}{2T}\right], \qquad (3\text{-}10)$$

then equation 3-9 becomes

$$\Delta c_{ok}(kT) = \frac{N(e(kT))}{M}K_f T. \qquad (3\text{-}11)$$

Since only the change in position between each error sample is of interest, equation 3-7 can be rewritten as

$$\Delta C_{ok}(s) = N(e(kT))[K_f/(Ms^2)]e^{-kTs} \qquad (3\text{-}12)$$

Equation 3-12 shows that the control pulse may be considered as a combination of a unit impulse and a nonlinearity having both dead zone and saturation regions. For this combination to accurately describe the forward transfer function of the control system, the transfer function G(s) must be multiplied by the gain multiplication factor, K_f.

As can be seen from equation 3-9, if the pulse duration time is small in comparison with twice the sampling period, i.e. $T_p \ll 2T$, then K_f can be approximated by T_p. This assumption will be used throughout most of this thesis. The position error that occurs during one sample period due to this approximation is shown graphically in Figure 2. Its effect on system stability is examined in the last two chapters.

The block diagram of Figure 1 is redrawn in Figure 3a using the previous approximations. In this diagram, the external force, $f_e(t)$, is assumed to act independently on the vehicle. The vehicle positions caused by the separate forces are summed to give the total position. This summation is justified because Laplace transforms are linear operators. The initial conditions, i.e. initial position and velocity, are applied to the mass upon which the external force acts.

The block diagram of Figure 3a is redrawn in parts b and c to show the equivalent Laplace and Z transform diagrams.

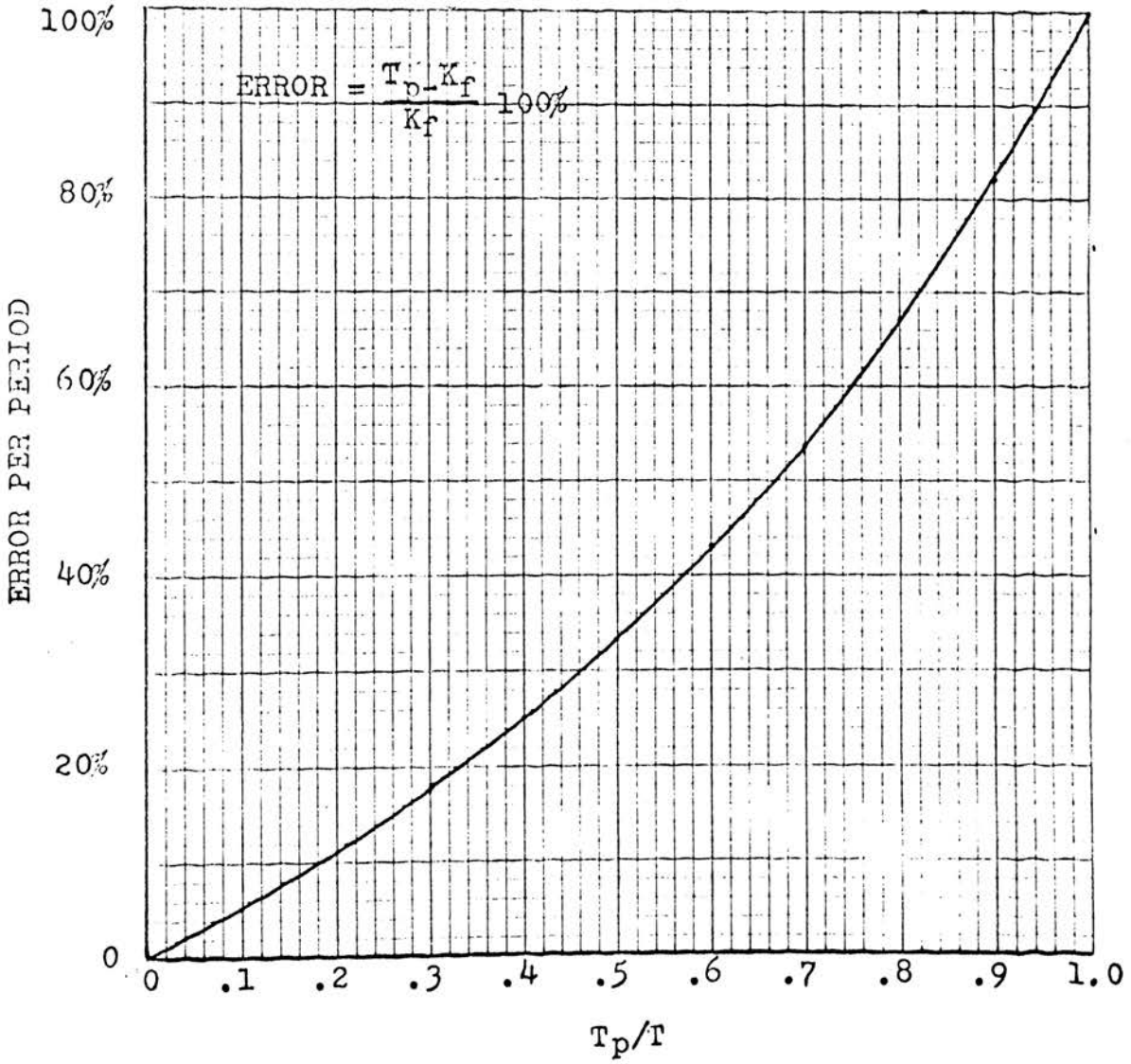

Figure 2. Error per period due to approximation that $K_f = T_p$.

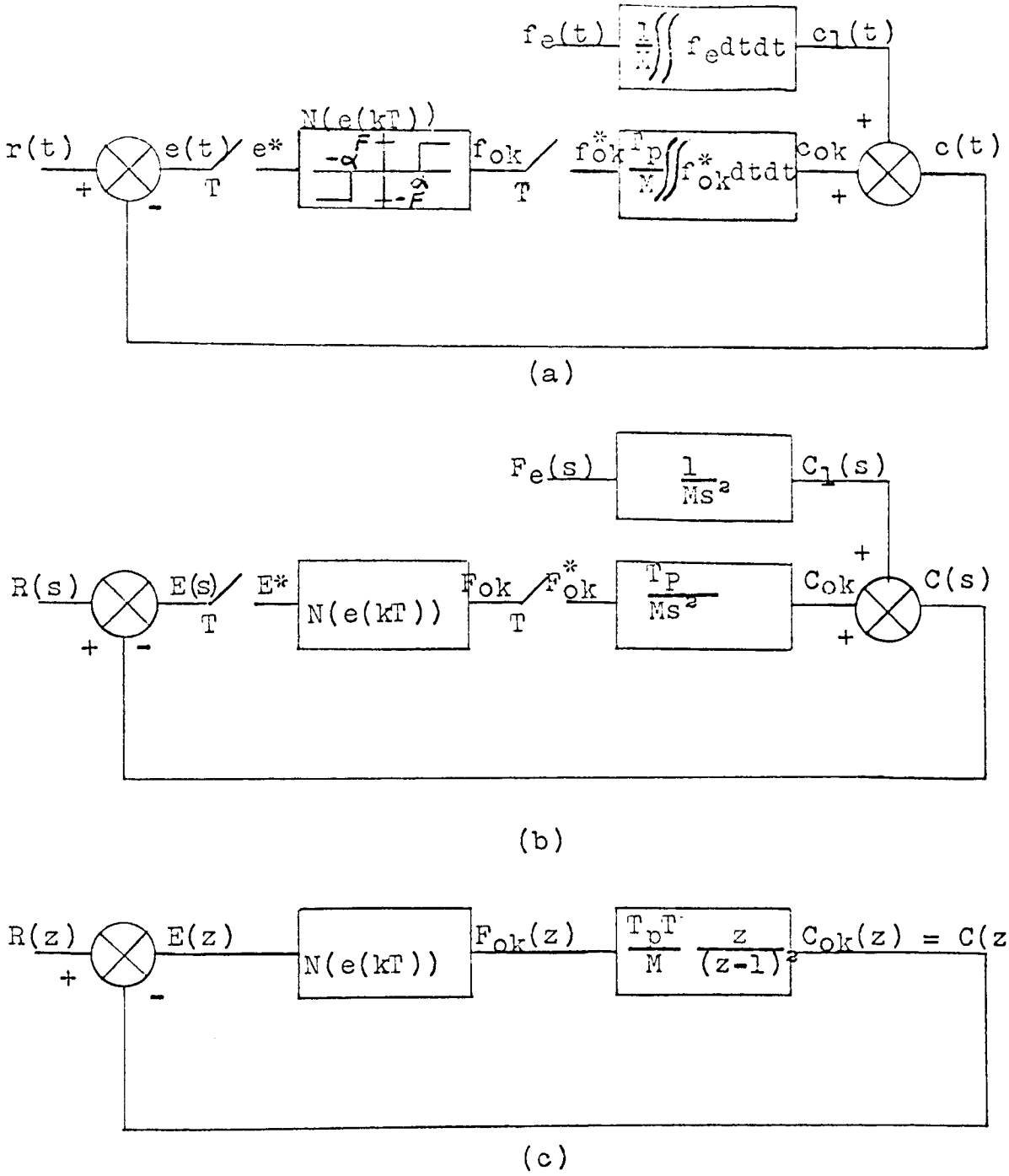

Figure 3. Control system block diagrams using impulse representation. a) Time equations b) Laplace transformed equations c) Z transformed equations with $f_e(t) = 0$.

The mathematical models of Figure 3 are used in the following chapters to analyze the control system.

Certain characteristics of the control system can be discerned from the block diagrams of Figure 3 and the preceeding equations. Consideration of the physical system shows that the use of the nonlinearity with saturation and dead zone regions and the unit impulse approximation is equivalent to an instantaneous change in velocity whenever the magnitude of the sampled error exceeds the dead zone limits. The change in velocity is given by the impulse-momentum equation using vehicle mass, thrust amplitude, and thrust duration time, i.e.

$$\Delta c'_{ok}(kT) = FT_p/M. \qquad (3\text{-}13)$$

Equation 3-13 gives an insight into the mechanics of the control system. The position is seen to be controlled by step changes in velocity in a direction to decrease the magnitude of the error signal.

CHAPTER IV

PHASE PLANE ANALYSIS

A number of techniques by which the stability of non-linear sampled data feedback control systems can be analyzed are available. These techniques include application of Popov's stability criterion, Lyapunov's second method, phase-plane analysis, and system simulation.

The first two methods of stability analysis mentioned above were attempted, but accurate conclusions could not be reached. Popov's stability (8) criterion provides sufficient, but not necessary, conditions for system stability. If these conditions are met, the conclusion that the system is stable can be drawn. However, if these conditions are not met, as was the case for the control system under study, no conclusion concerning system stability can be drawn.

Lyapunov's second method (9) provides necessary and sufficient conditions for stability. However, application of the method is contingent upon one's ability to derive a proper Lyapunov function from the system's state equations. The author was not able to apply this method of analysis.

Phase-plane diagrams, often used as an analysis technique, proved to be applicable to the study of the control system defined in the previous chapter. Truxal (10) explains the technique of applying this type of analysis to continuous systems. Aseltine (11) and Lindorff (8,12) use difference equations to develop incremental phase-plane

analysis techniques which may be applied to nonlinear sampled data control systems. This chapter develops the incremental phase-plane techniques which apply to the nonlinear sampled data control system as shown in Figure 3 and uses these techniques to determine the system's general response characteristics.

If the change in variables indicated by Lindorff (8,12) is now made, the block diagram shown in Figure 3c can be manipulated into the form shown in Figure 4. It should be noted that the two diagrams are exactly equivalent only when K=1. A value of $K \neq 1$ is shown in Chapter V to be equivalent to employment of a compensator in the system.

The equations which describe the system where K=1 can now be written directly from the diagram of Figure 4. If the input signal is zero, i.e. R(z) = 0, these equations are written as

$$(z-1)^2X(z) = -[T_pT/M]F_{ok}(z), \tag{4-1}$$

$$(z-1)X(z) = Y(z), \tag{4-2}$$

and

$$E(z) = KY(z) + X(z). \tag{4-3}$$

The equation for the first forward difference is defined (8,9,11) as follows

$$\Delta x(kT) = x(kT+T) - x(kT). \tag{4-4}$$

The second forward difference is defined as

$$\begin{aligned}\Delta^2 x(kT) &= \Delta(\Delta x(kT)) = \Delta x(kT+T) - \Delta x(kT) \\ &= x(kT+2T) - 2x(kT+T) + x(kT).\end{aligned} \tag{4-5}$$

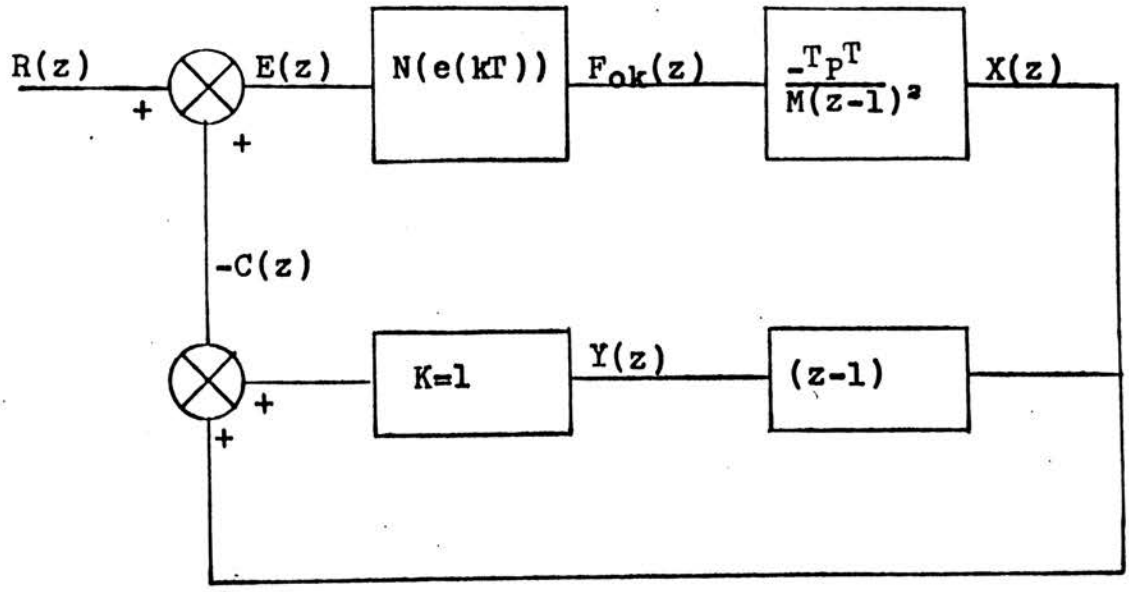

Figure 4. Control system block diagram showing change in variable for the uncompensated system.

Recalling that if initial conditions are neglected,

$$Z[x(kT)] = X(z) \tag{4-6}$$

and

$$Z[x(kT+T)] = zX(z), \tag{4-7}$$

the Z transforms of equations 4-4 and 4-5 are

$$Z[\Delta x(kT)] = (z-1)X(z) \tag{4-8}$$

and

$$Z[\Delta^2 x(kT)] = [z^2-2z+1]X(z)$$
$$= (z-1)^2X(z). \tag{4-9}$$

Therefore, the inverse Z transforms of equations 4-1 through 4-3 can be rewritten as

$$\Delta^2 x(kT) = -[T_pT/M]f_{ok}(kT) \tag{4-10}$$

$$\Delta x(kT) = y(kT) \tag{4-11}$$

$$e(kT) = Ky(kT) + x(kT). \tag{4-12}$$

Substituting equation 4-11 in 4-10, one gets

$$\Delta(\Delta x(kT)) = \Delta y(kT) = -[T_pT/M]f_{ok}(kT) \tag{4-13}$$

and dividing equation 4-13 by equation 4-11, one gets

$$\frac{\Delta y(kT)}{\Delta x(kT)} = -[T_pT/M]\frac{f_{ok}(kT)}{y(kT)} = K_2 \quad . \tag{4-14}$$

Equation 4-14 is the equation for the isoclines in an incremental phase-plane whose coordinates are x and y (x and Δx). The trajectories are easy to plot since they are composed of straight line segments. The slopes of these segments are given by equation 4-14 and change in the x coordinates is given by equation 4-11.

If the y coordinate at the kth sampling instant is zero ($y(kT) = 0$), the slope of the trajectory is infinite as

shown by equation 4-14. Equation 4-13 can then be solved to obtain the change in the y coordinate as

$$\Delta y(kT) = y(kT+T) - y(kT) = -[T_pT/M]f_{ok}(kT)$$

and, therefore,

$$y(kT+T) = -[T_pT/M]f_{ok}(kT). \tag{4-15}$$

The value of $f_{ok}(kT)$ is a factor in equation 4-14 which gives the isoclines and slope of the trajectories. The value of $f_{ok}(kT)$ is given by equations 3-2 and 3-3. Combining these equations one obtains

$$f_{ok}(kT) = \begin{cases} F & , e(kT) \geq \alpha \\ 0 & , |e(kT)| < \alpha \\ -F & , e(kT) \leq \alpha \end{cases} \tag{4-16}$$

Equations 4-16 and 4-12 may be combined to give the equations for the switching curves in the incremental phase-plane. The equations for the switching curves are

$$Ky(kT) + x(kT) = \alpha \tag{4-17}$$

and

$$Ky(kT) + x(kT) = -\alpha \tag{4-18}$$

For the uncompensated feedback control system, i.e. K=1, the above equations become

$$y(kT) + x(kT) = \alpha \tag{4-19}$$

and

$$y(kT) + x(kT) = -\alpha. \tag{4-20}$$

Throughout the remainder of this chapter, the phase-planes are drawn using the assumption that T = 1 sec and FT_p/M = 1 unit distance per second. Although these values would never be used in an actual system, they will yield trajectories which show the system's general characteristics.

It will be obvious from the trajectories that the use of these values has little effect on the amplitude characteristics of the system, but that they act as a time scaling to speed up the response of the system. The advantage to using these values is in simplification in construction of the phase-plane trajectories. This is easily seen since equation 4-14 now becomes

$$K_2 = \frac{\Delta y(kT)}{\Delta x(kT)} = - \frac{\text{sgn}[f_{ok}(kT)]}{y(kT)} , \qquad (4\text{-}21)$$

and equation 4-15 becomes

$$y(kT+T) = -\text{sgn}[f_{ok}(kT)]. \qquad (4\text{-}22)$$

The incremental phase-plane in Figure 5 illustrates the simplicity entailed in its construction. Figures 6 and 7 show phase-plane trajectories for several values of dead zone (allowable error).

These figures show several important characteristics of the control system. The most important item is that for the uncompensated control system (K=1) a stable limit cycle exists for every set of starting values. Thus the origin is seen to be a "center" (9,10).

The existence of stable limit cycles for the uncompensated system is a reasonable solution if one recalls the discussion of the system's physical characteristics at the end of Chapter 3. Quoting from page 13,

> "The position is seen to be controlled by step changes in velocity in a direction to decrease the magnitude of the error signal."

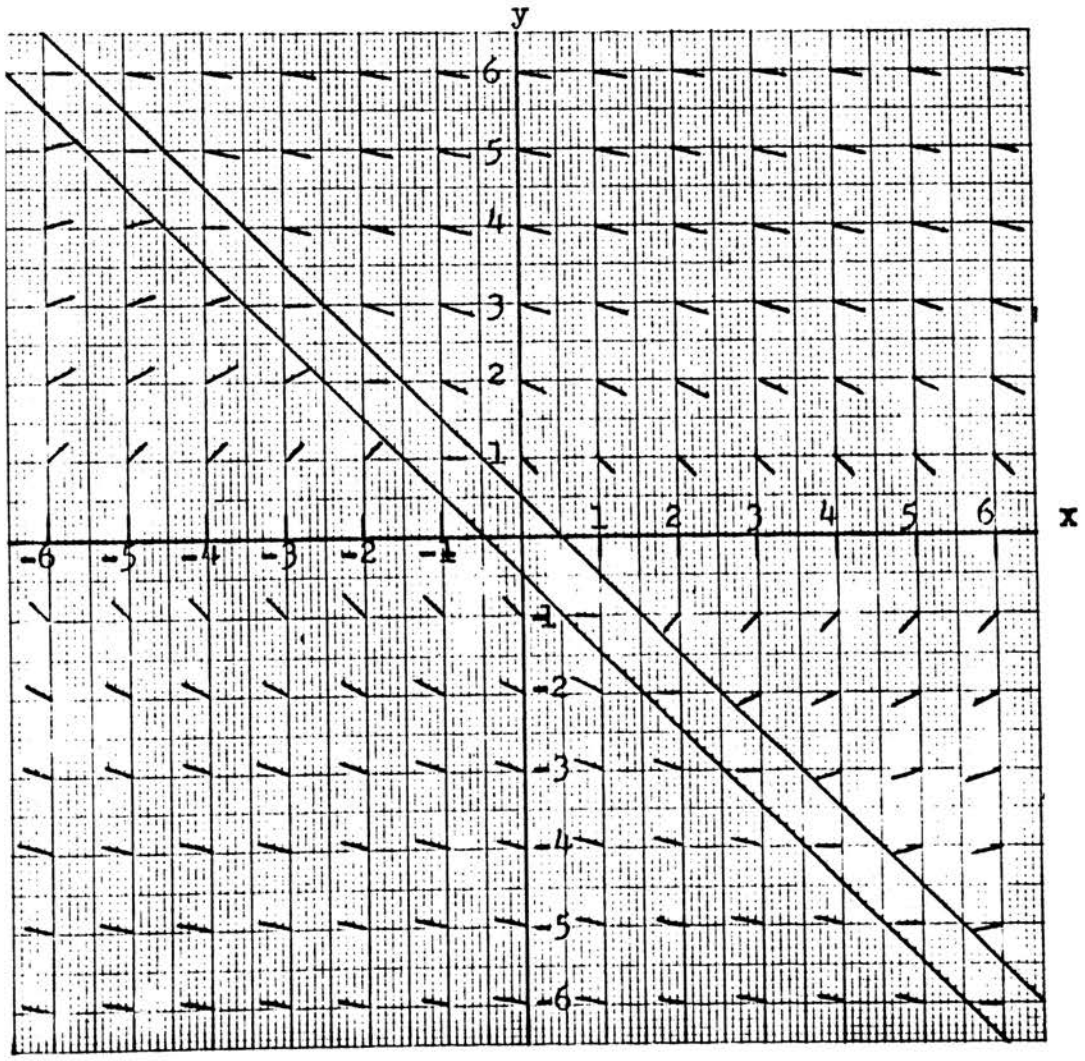

Figure 5. Phase-plane showing trajectory slopes and switching lines for $\alpha = 0.5$.

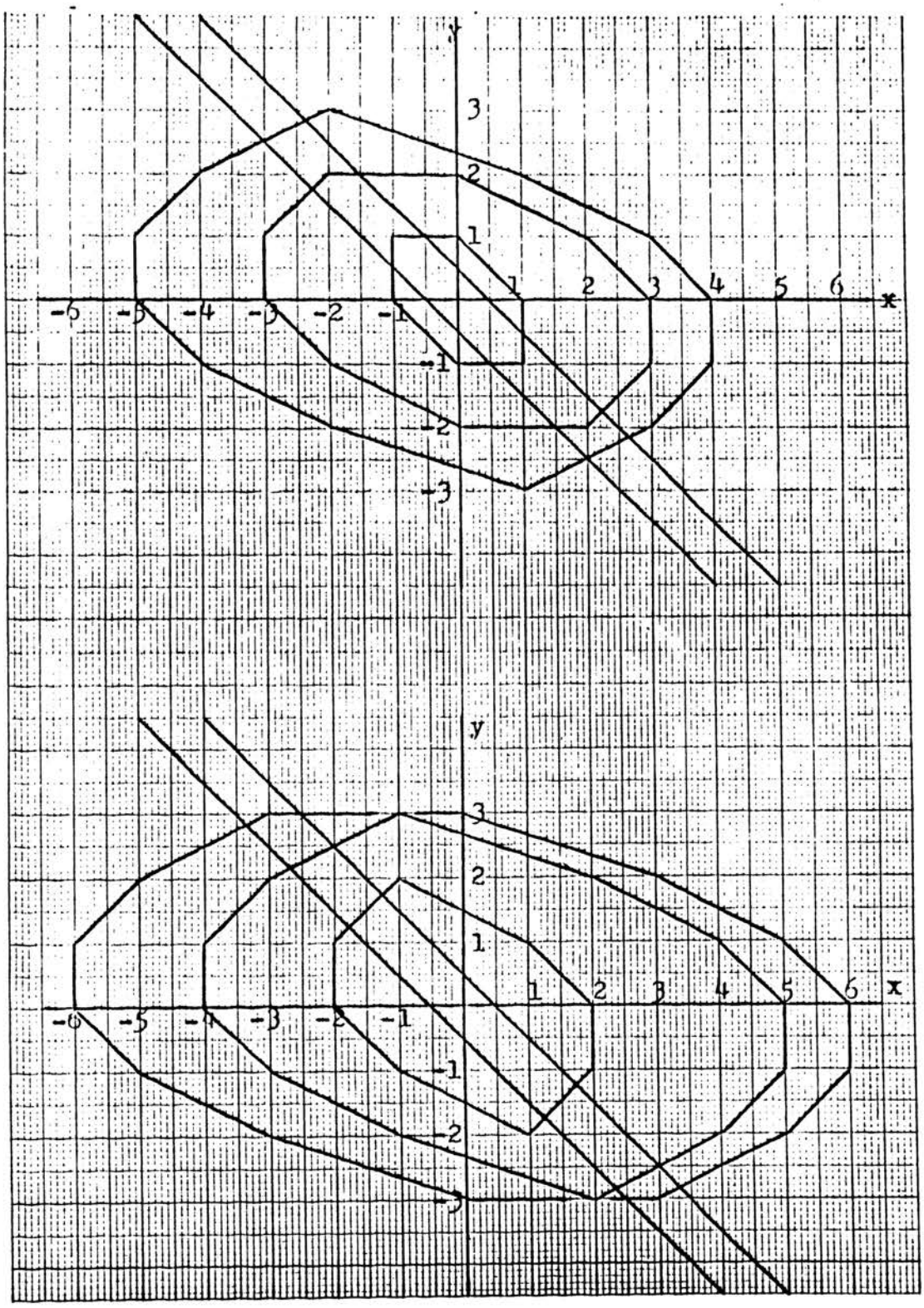

Figure 6. Phase-plane trajectories for the uncompensated system with $\alpha = 0.5$.

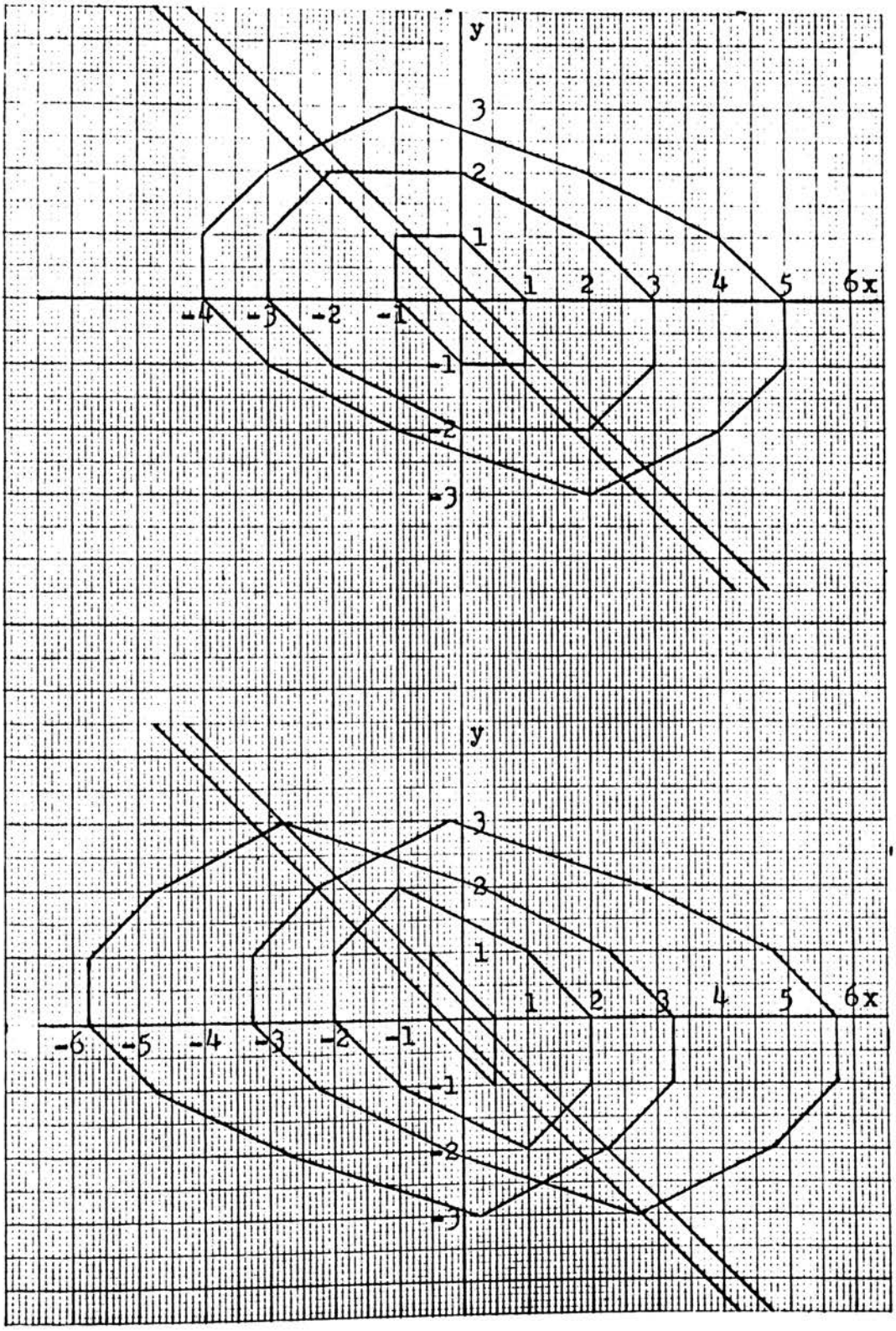

Figure 7. Phase-plane trajectories for the uncompensated system with $\alpha = 0.25$.

Since the uncompensated system acts only on error magnitude information (no rate feedback), there is an equal number of velocity steps for positive and negative values of error. Thus, the position of the system is seen to always return through its starting position.

The second noticeable item seen in Figures 6 and 7 is that the period of each limit cycle oscillation depends upon the amplitude of the starting position and upon the value of dead zone.

The correspondence between the starting position in the phase-plane and the initial conditions of velocity and position is shown below with the aid of Figure 8. From this figure, one sees that

$$\frac{C(z)}{F_{ok}(z)} = Z\left[\frac{T_p}{M}\frac{1}{s^2}\right] = \frac{T_pT}{M}\frac{z}{(z-1)^2} \qquad (4\text{-}23)$$

and

$$\frac{C'(z)}{F_{ok}(z)} = Z\left[\frac{T_p}{M}\frac{1}{s}\right] = \frac{T_p}{M}\frac{z}{(z-1)} \qquad (4\text{-}24)$$

Therefore,

$$\frac{X(z)}{F_{ok}(z)} = K_3\left[\frac{T_p}{M}\frac{z}{(z-1)}\right] - K_4\left[\frac{T_pT}{M}\frac{z}{(z-1)^2}\right]$$

$$= \frac{T_p}{M}\left[\frac{K_3z(z-1) - K_4Tz}{(z-1)^2}\right]. \qquad (4\text{-}25)$$

Rewriting equation 4-1, one gets

$$\frac{X(z)}{F_{ok}(z)} = \frac{T_p}{M}\left[\frac{T}{(z-1)^2}\right]. \qquad (4\text{-}26)$$

Equating 4-25 and 4-26, one obtains

$$K_3z(z-1) - K_4Tz = -T$$

or

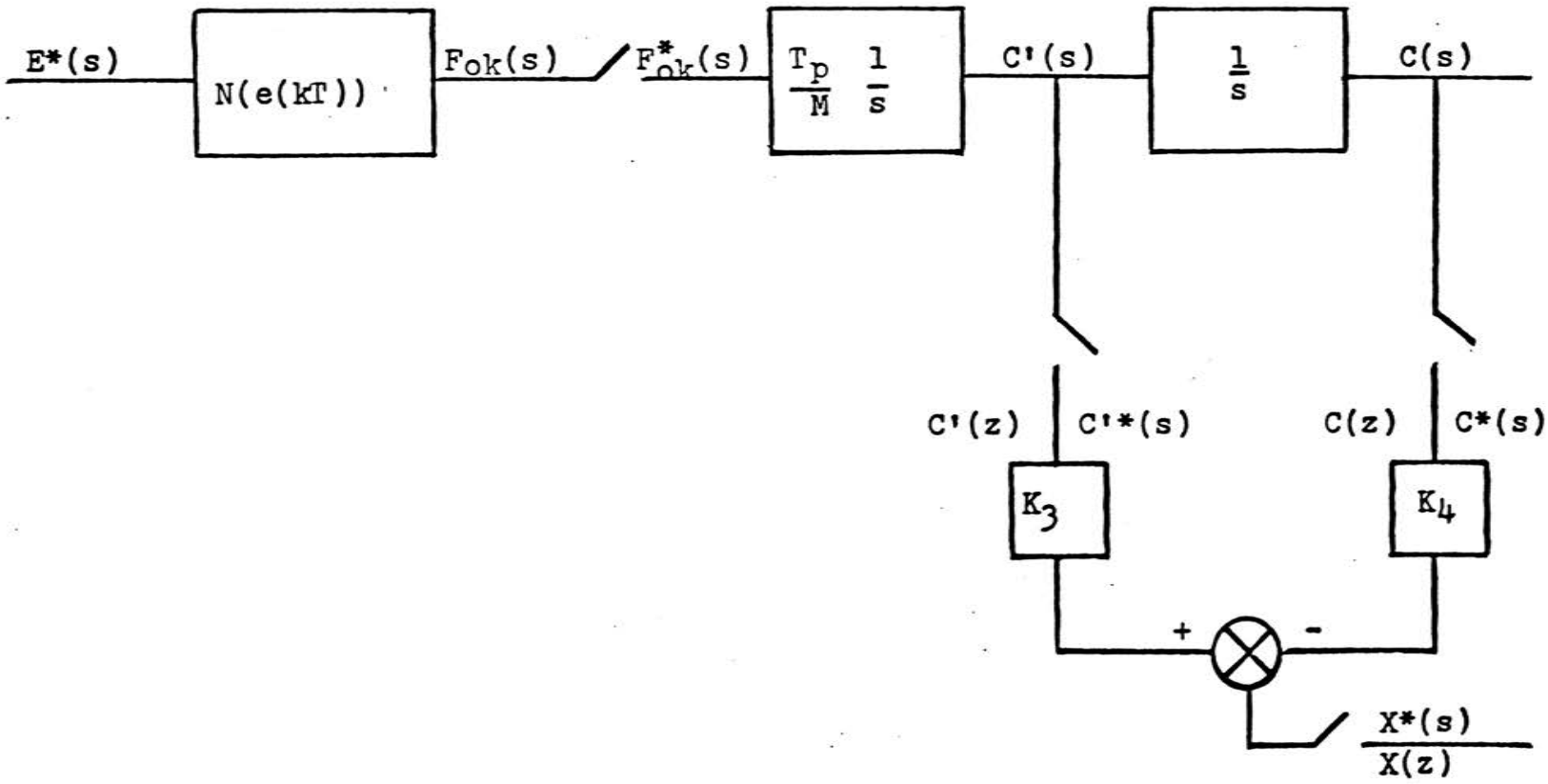

Figure 8. Generation of X(z) from C'(z) and C(z).

$$K_3 z^2 - z(K_3+K_4T) = -T. \quad (4\text{-}27)$$

Equation 4-27 is satisfied if

$$K_3 = Tz^{-1}$$

and

$$K_4 = 1.$$

From Figure 8,

$$X(z) = K_3C'(z) - K_4C(z)$$

$$= Tz^{-1}C'(z) - C(z). \quad (4\text{-}28)$$

The inverse Z transform yields the time solution

$$x(kT) = Tc'(kT-T) - c(kT). \quad (4\text{-}29)$$

For initial conditions, t is equal to zero. Therefore,

$$x(0) = Tc'(-T) - c(0) \quad (4\text{-}30)$$

For the unforced system, $c'(-T)$ equals $c'(0^-)$. The minus sign is used to indicate the value of $c'(t)$ as $t \to 0$ from the negative direction. This designation is needed because if the error exceeds its dead zone limit ($|e| > \alpha$), a step change in velocity will occur at t=0. Thus, $c(0^-)$ need not be equal to $c(0^+)$. Using this designation, equation 4-30 becomes

$$x(0) = Tc'(0^-) - c(0) \quad (4\text{-}31)$$

Recalling that for the unforced, uncompensated system $e(kT)$ equals $-c(kT)$ and K equals 1, equation 4-12 can be written as

$$c(kT) = -y(kT) - x(kT). \quad (4\text{-}32)$$

Substituting equation 4-29 in 4-32, one obtains

$$y(kT) = -Tc'(kT-T). \quad (4\text{-}33)$$

For the reasons given above, this equation becomes

$$y(0) = -Tc'(0^-). \qquad (4\text{-}34)$$

The initial conditions as transformed to the phase-plane variables are therefore given by equations 4-31 and 4-34. These equations show that the x axis of the phase-plane corresponds to sets of initial conditions whose initial velocities are all zero. Thus, trajectories whose initial conditions lie along this axis are solutions to the control system for step inputs.

The value of the error at any sample time t = kT can be read directly from the phase-plane trajectory as the sum of the coordinates (equation 4-12). For the absence of an input signal (r(t) = 0), the position is the negative of the sum of the coordinates (equation 4-32). The velocity just previous to each sample time is the negative of the y coordinate (equation 4-33).

The position values which correspond to the previous phase-plane trajectories, Figures 6 and 7, are plotted in Figures 9 and 10 respectively. These graphs are the solutions for a system with various values of step input signal.

These graphs clearly illustrate the conclusions drawn from the original phase-plane trajectories. That a stable limit cycle exists for each set of initial conditions is evident. The effect of initial condition amplitude and dead zone limits on the period of an oscillation is also clear.

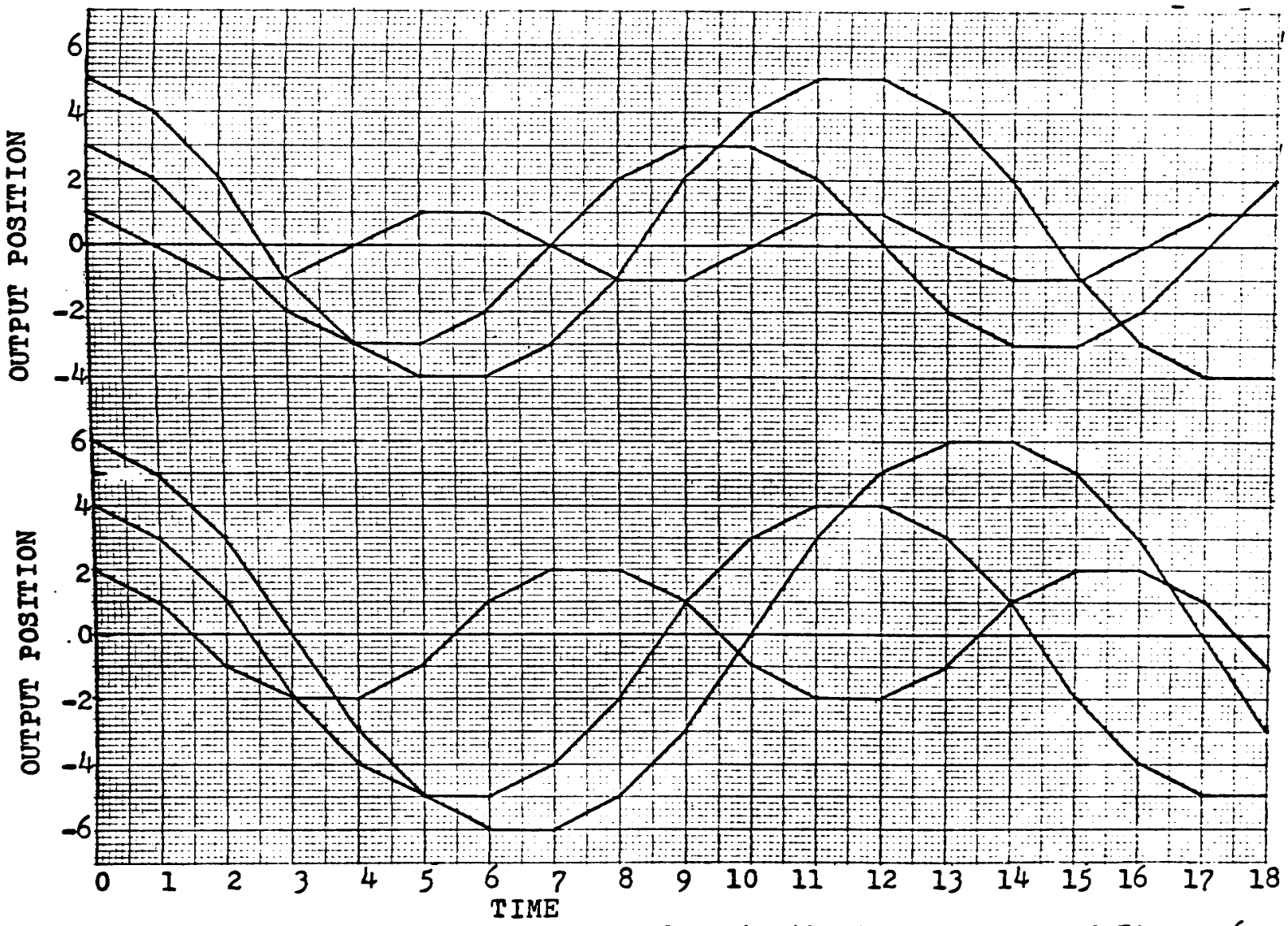

Figure 9. Output position values corresponding to the trajectories of Figure 6.

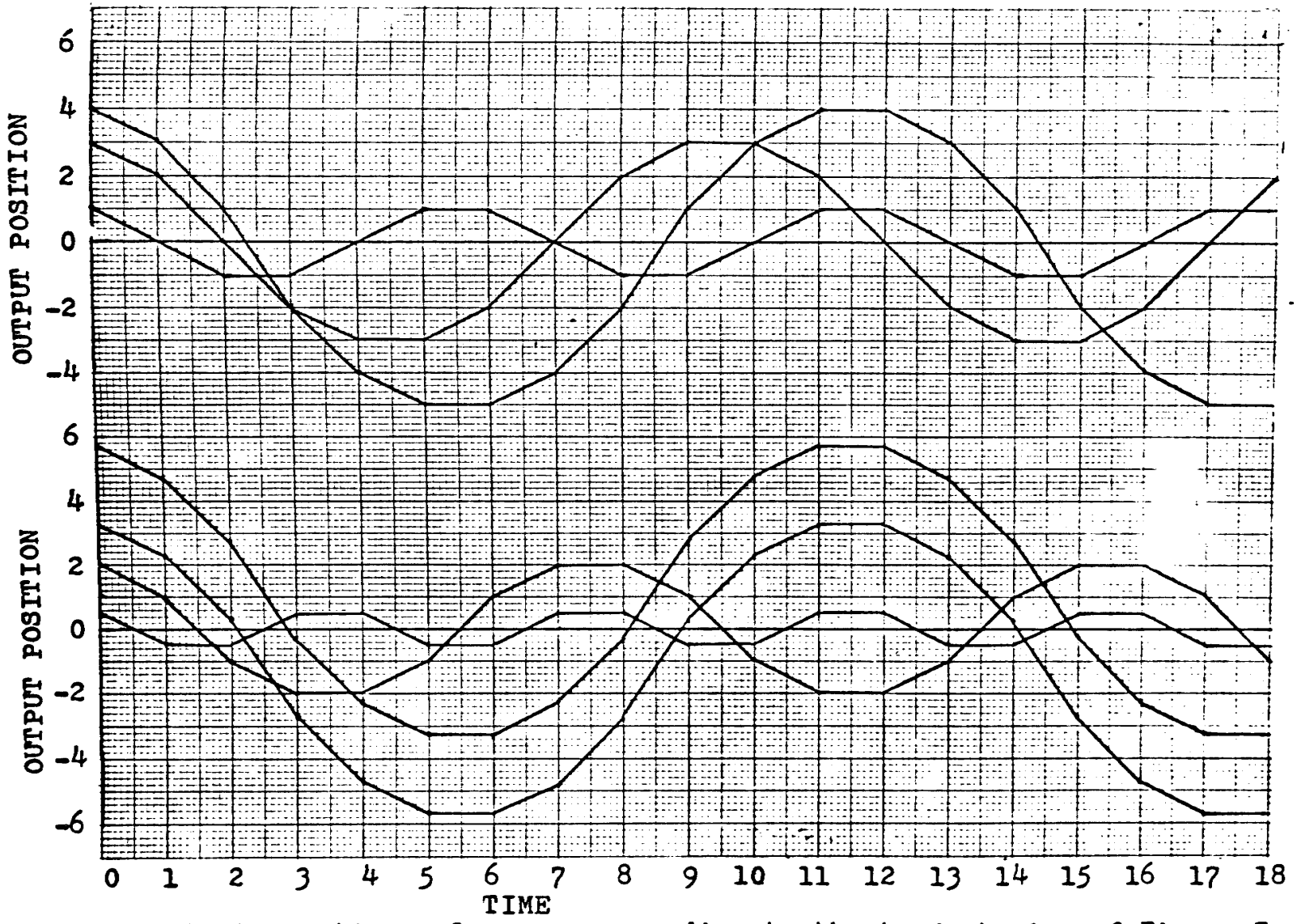

Figure 10. Output position values corresponding to the trajectories of Figure 7.

The incremental phase-plane analysis can be extended to analyze the control system for simple input signals. From Figure 4, the equation for E(z) can be written as

$$E(z) = R(z) - C(z). \tag{4-35}$$

Taking the inverse Z transform,

$$e(kT) = r(kT) - c(kT). \tag{4-36}$$

Substituting equation 4-32 in 4-36, one gets

$$e(kT) = r(kT) + y(kT) + x(kT), \tag{4-37}$$

and, therefore,

$$\Delta e(kT) = \Delta r(kT) + \Delta y(kT) + \Delta x(kT). \tag{4-38}$$

From equation 4-38, one sees that the trajectory in the incremental phase-plane with coordinates x and y is equivalent to a plot of the sampled error if the increment $\Delta r(kT)$ is added algebraically at each point $t = kT$.

The initial conditions as transformed to the phase-plane can be obtained by slight modification of equations derived on page 25. These equations now become

$$x(0) = Tc'(0^-) - c(0) + r(0) \tag{4-39}$$

and

$$y(0) = -Tc'(0^-). \tag{4-40}$$

The equations derived in the previous section hold for any input signal r(t). However, as is seen from equation 4-38, the value of $\Delta r(t)$ must be known or calculated at every instant of time $t = kT$.

The input signal which is most easily analyzed is the ramp given by

$$r(t) = At + r(0). \tag{4-41}$$

In applying this signal, one sees that

$$\Delta r(kT) = AT = \text{a constant.}$$

The analysis of the control system for the value of AT equal to -0.5 and several different initial conditions is shown in Figure 11. The corresponding time plots of the error and of the position are shown in Figures 12 and 13, respectively.

This analysis of the system for the ramp input shows that the output position does follow the input, but that it also continues to display stable limit cycle oscillation.

Since slowly varying signals can be approximated by piece-wise linear signals (ramp signals), the above conclusions can be extended to include various other input signals. For instance, if the input signal is sinusoidal, many piece-wise linear signals will be needed for a good approximation. Therefore, the period of the sinusoidal signal must be much greater than the sampling period. The amplitude of the input sinusoidal signal also influences the ability of the output of the control system to follow it since the nonlinearity possesses a saturation region.

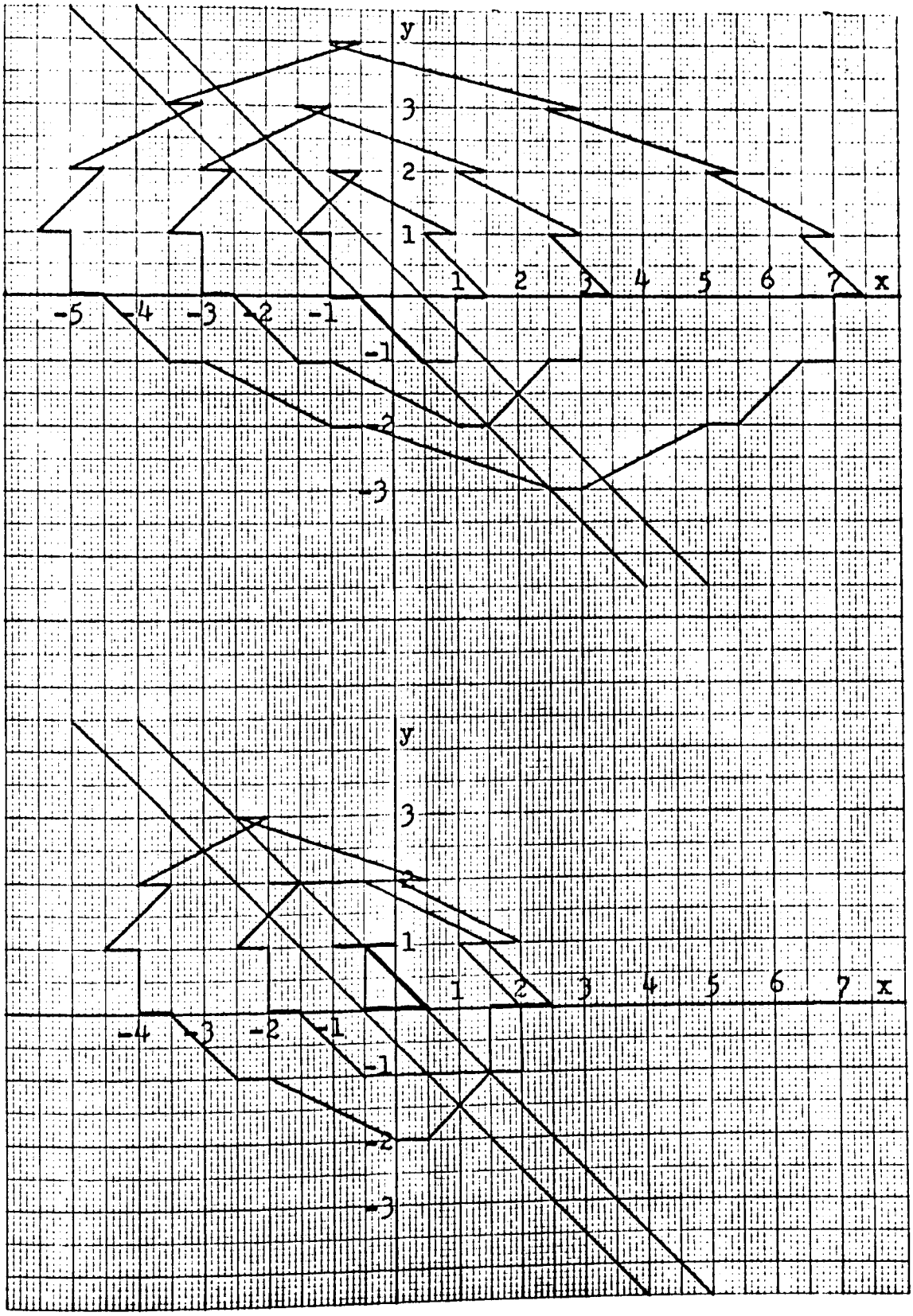

Figure 11. Phase-plane trajectories for the uncompensated system with $\alpha = 0.5$ and a ramp input with A=-.5.

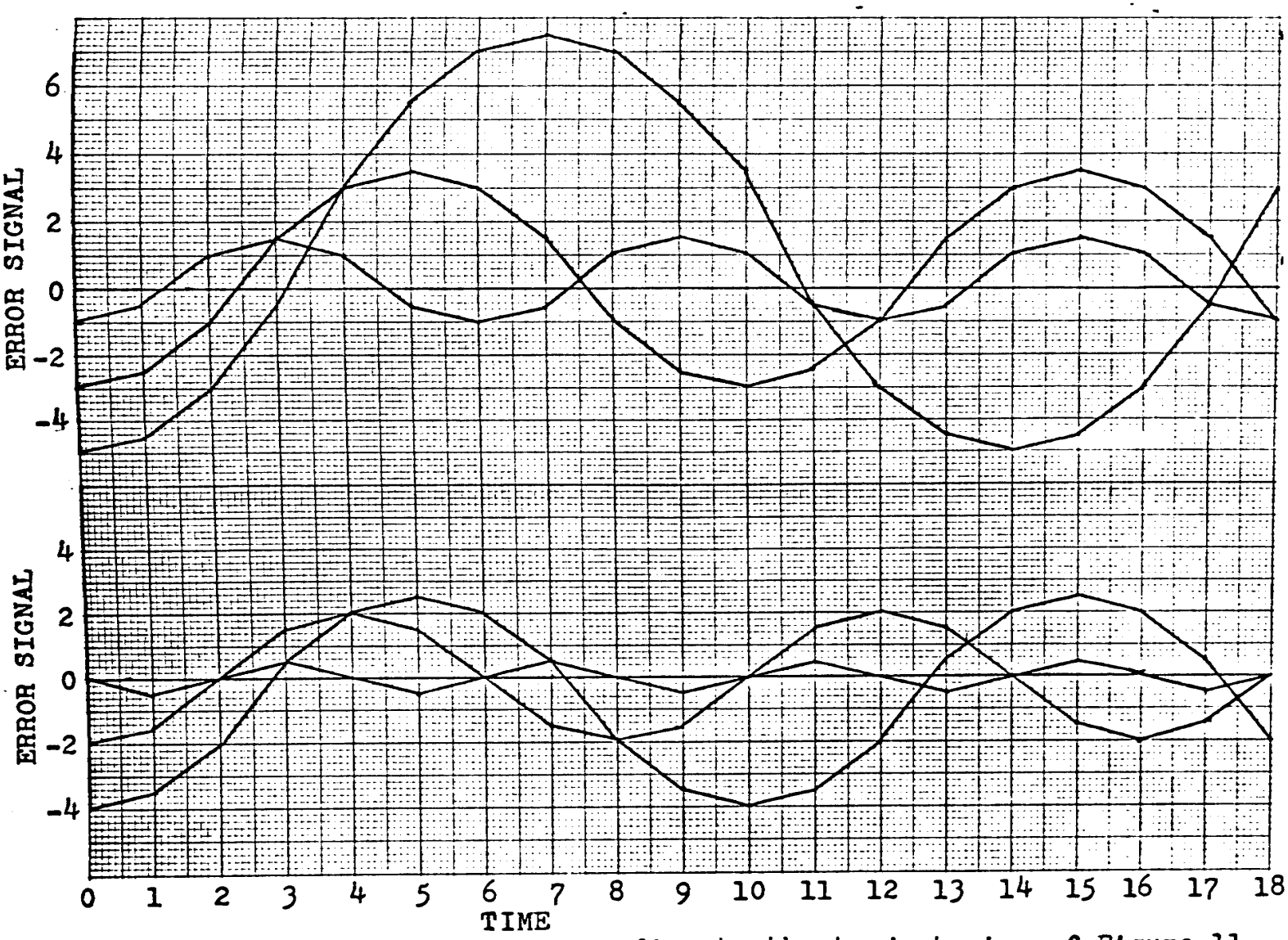

Figure 12. Error signal values corresponding to the trajectories of Figure 11.

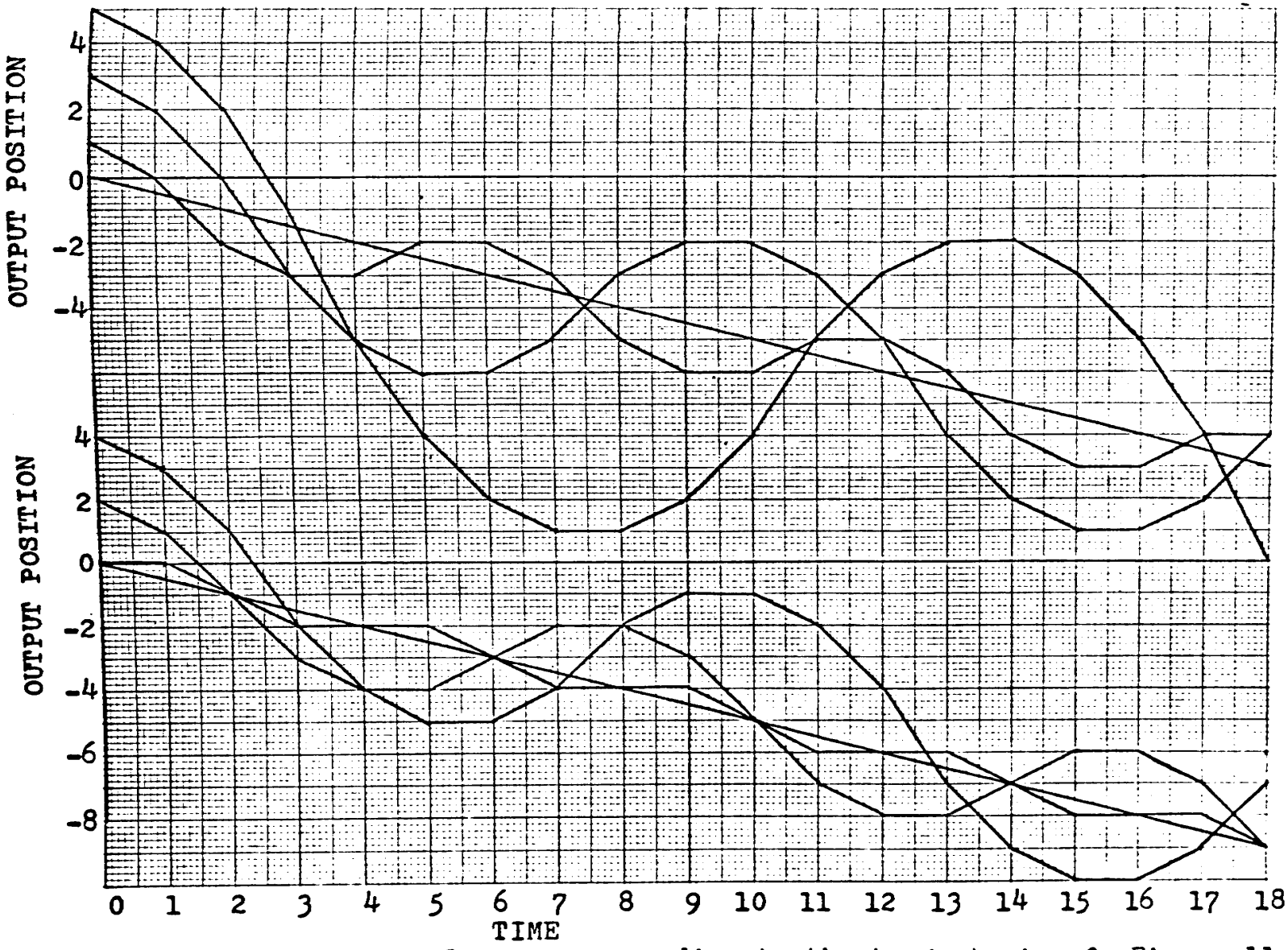

Figure 13. Output position values corresponding to the trajectories fo Figure 11.

CHAPTER V

PHASE PLANE COMPENSATION DESIGN

The uncompensated nonlinear sampled data feedback control system described mathematically in Chapter III was analyzed in Chapter IV. It was found to possess a stable limit cycle corresponding to each set of initial conditions. These oscillations also were found to exist for the ramp input signal.

This chapter studies the system using a specific type of compensation element, namely an element which corresponds to a value of gain $K \neq 1$.

Equations 4-17 and 4-18, repeated below, are the general equations for the switching curves in the incremental phase-plane.

$$Ky(kT) + x(kT) = \alpha \tag{5-1}$$

$$Ky(kT) + x(kT) = -\alpha \tag{5-2}$$

The compensated system with no input signal ($r(t) = 0$) is considered first in this analysis. Therefore, equation 4-12 applies since $e(kT)$ becomes $e_2(kT)$ as is seen from comparison of Figures 4 and 14. Equation 4-32 also applies. These equations are repeated below.

$$e_3(kT) = Ky(kT) + x(kT) = e_2(kT) \tag{5-3}$$

$$c(kT) = -y(kT) - x(kT) = -e(kT) \tag{5-4}$$

At this point in the analysis, it becomes necessary to consider the coordinates of the phase-plane. From equations 5-3 and 5-4, it appears that these coordinates could be

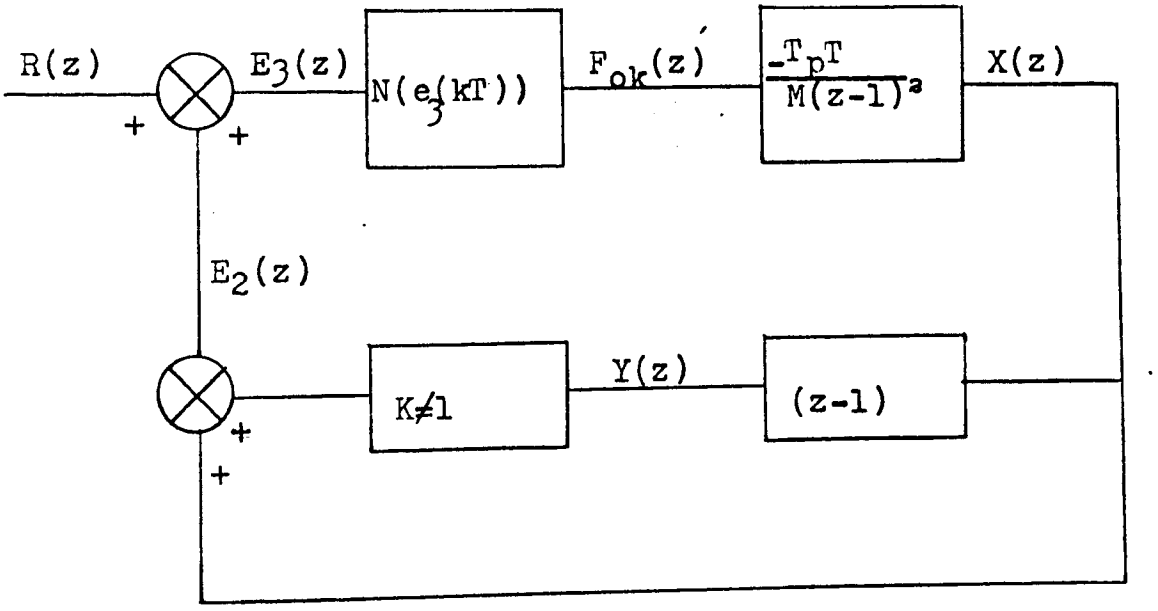

Figure 14. Control system block diagram showing change in variable for the compensated system.

either Ky vs x or y vs x. However, if the former is chosen, the equations for the initial condition transformations, equations 4-31 and 4-34 are no longer valid. Therefore, the phase-plane coordinates y and x are also used in this chapter.

It should be noted that the output position can be read directly from the phase-plane trajectories as shown by equation 5-4; but the compensation error signal is not easily obtained unless the values of Ky are also shown along the y axis.

Phase-plane trajectories corresponding to values of gain, K, of 5.0, 2.0, and 1.5 are shown in Figures 15, 16, and 17. Figures 15 and 16 show that the trajectories converge to a limit cycle of small amplitude or to a small average value. These results are clearly indicated by the output position plots of Figures 18 and 19 which correspond to representative trajectories of Figures 15 and 16 respectively.

The existence of a small amplitude limit cycle is an expected result since the nonlinearity in the forward path possesses a dead zone region. The amplitude of the oscillation shown in these figures is equal to the dead zone limits.

A very interesting phenomena is displayed by several trajectories shown in Figure 17. These trajectories indicate that large amplitude oscillations may exist for certain particular initial conditions even though the

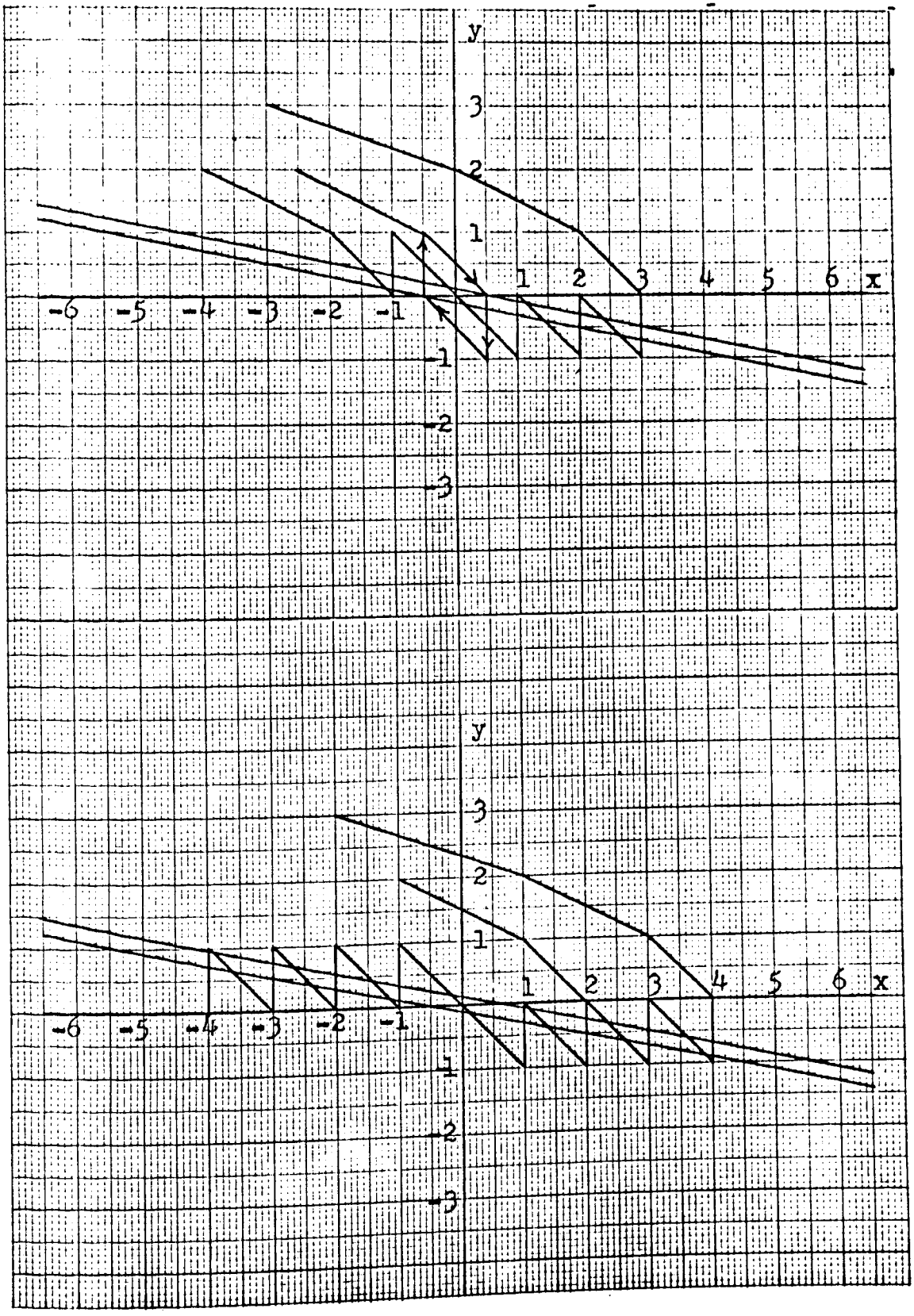

Figure 15. Phase-plane trajectories for the compensated system with $K=5$ and $\alpha=0.5$.

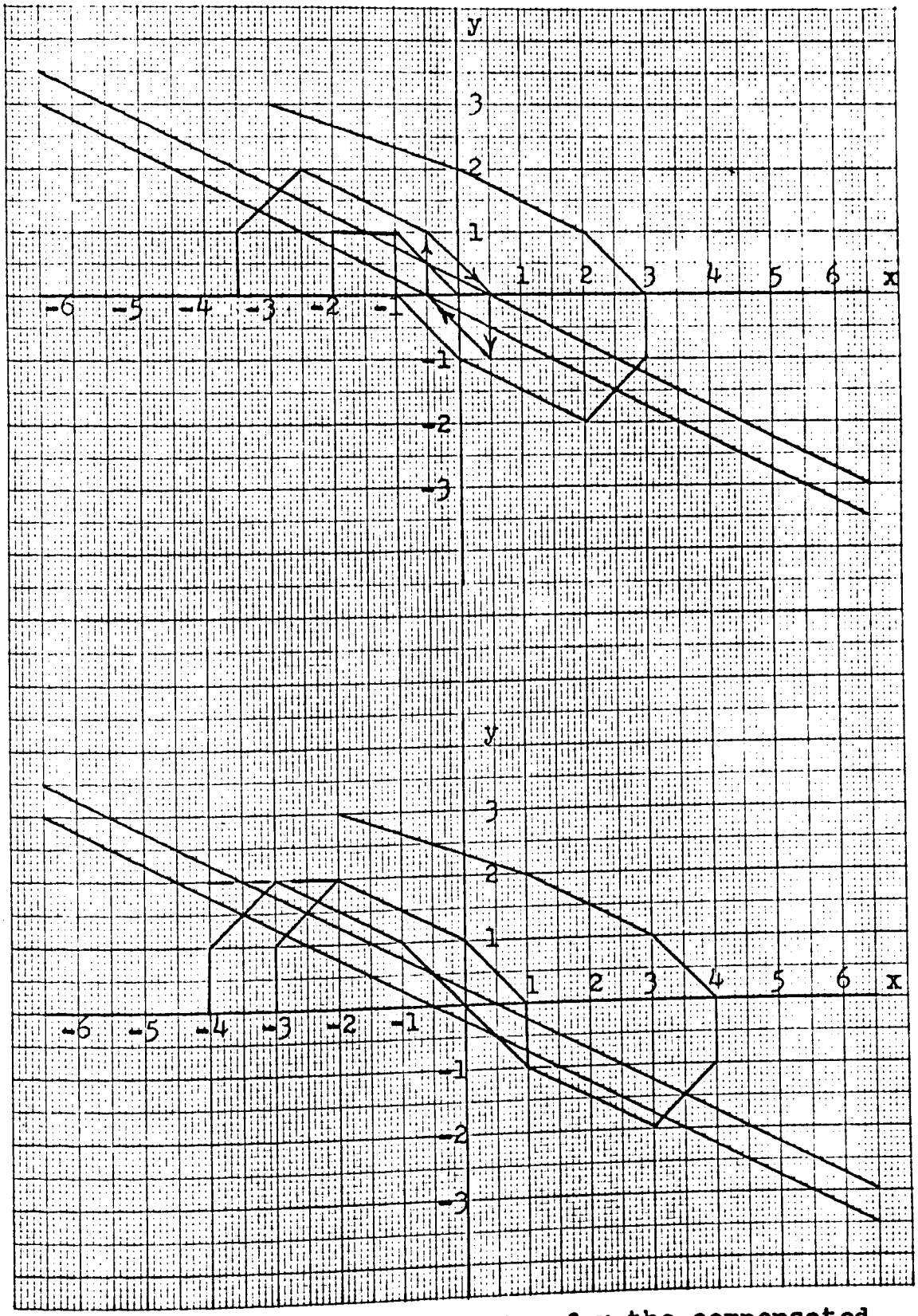

Figure 16. Phase-plane trajectories for the compensated system with K=2 and α=0.5.

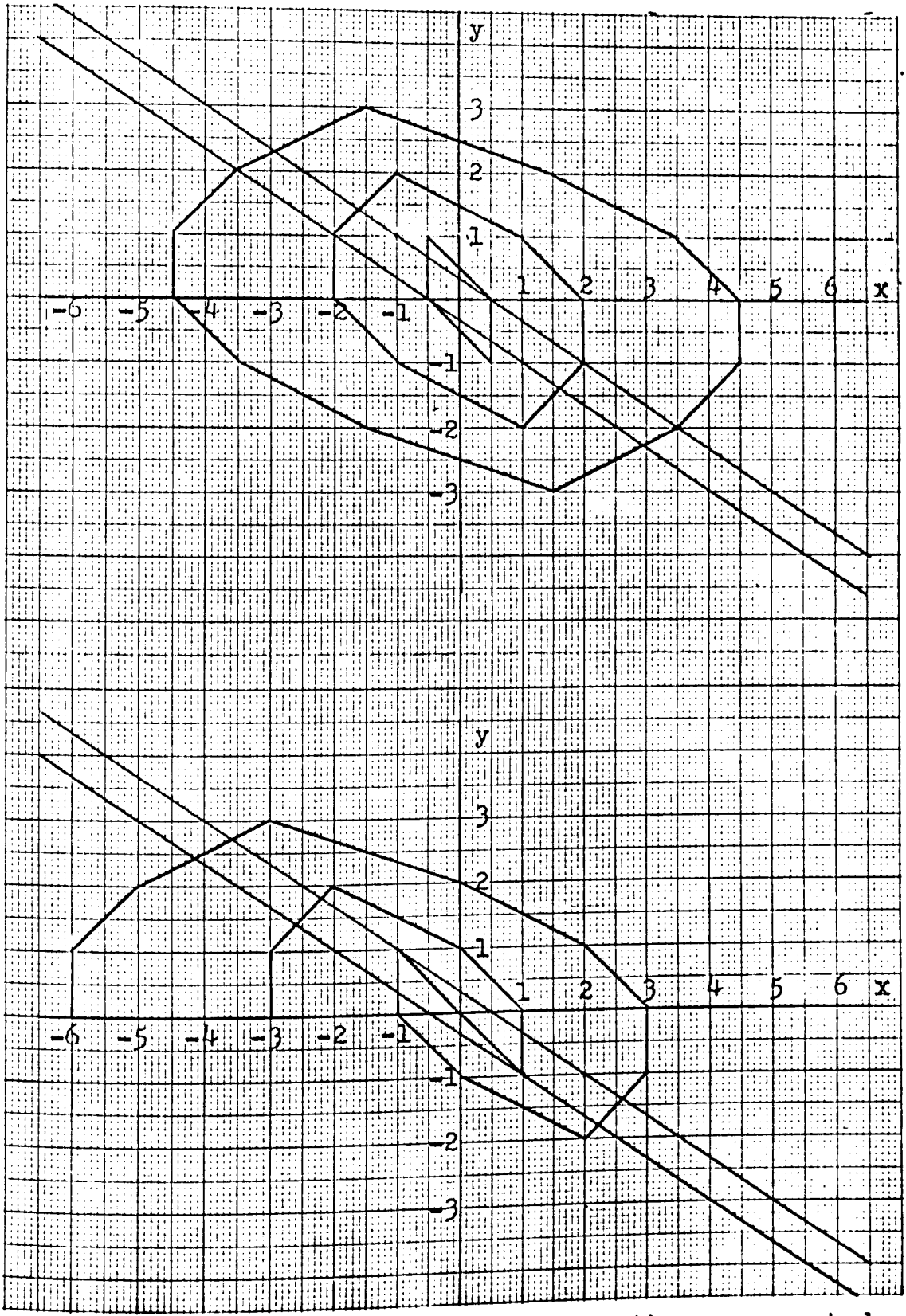

Figure 17. Phase-plane trajectories for the compensated system with K=1.5 and α=0.5.

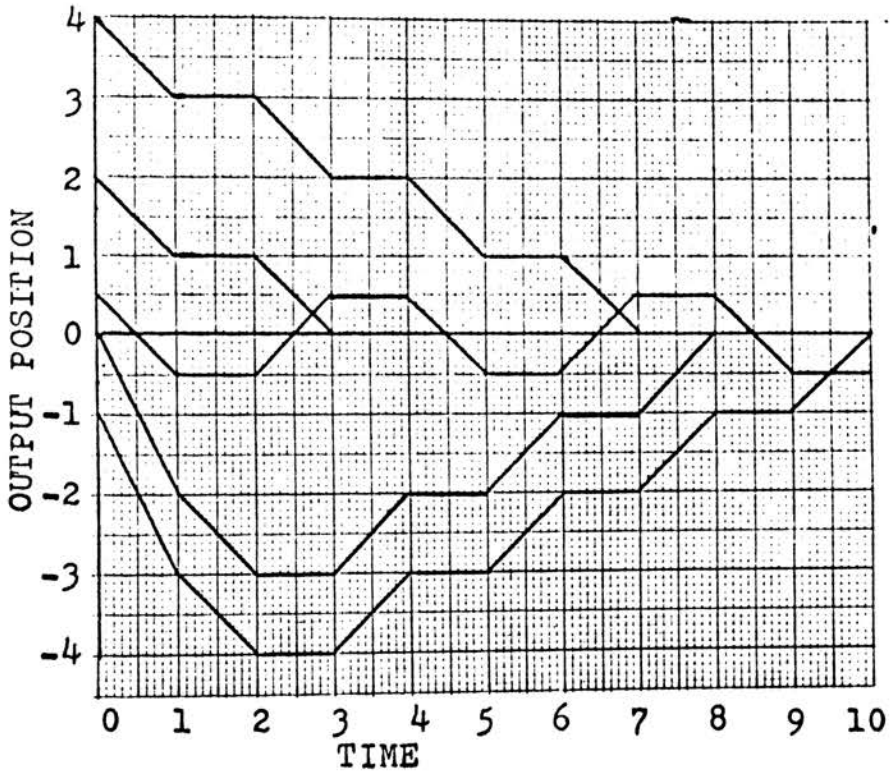

Figure 18. Output position values corresponding to the trajectories of Figure 15.

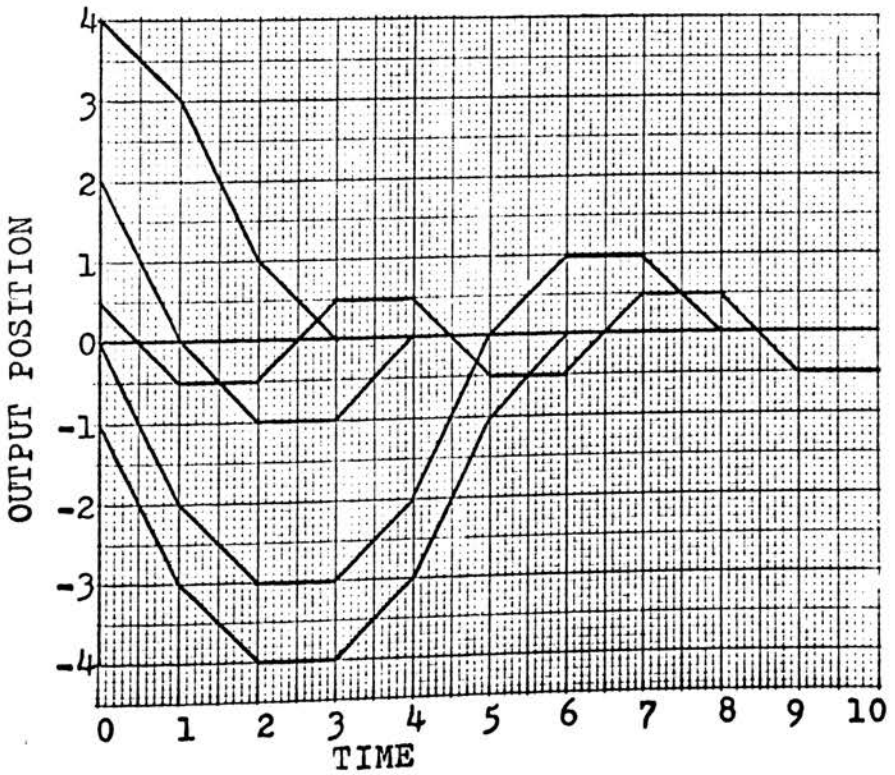

Figure 19. Output position values corresponding to the trajectories of Figure 16.

system has been compensated. However, contrary to the characteristics of most continuous phase-planes, trajectories starting at initial conditions lying within the boundaries of these stable limit cycles do not necessarily converge to either of these limit cycles. Trajectories which originate at these general points may converge to the expected small amplitude limit cycle.

Even though theoretically these undesirable limit cycles can be shown to exist, in an actual physical system they probably would not be present. This is true since for their existence the trajectories must possess particular values at the sampling instants $t = kT$. However, due to the presence of external forces acting on the vehicle, and noise in the sampling mechanism, the values of sampled error will lie only in the neighborhood of the required particular values and, therefore, these trajectories should converge to the expected minimal limit cycle.

The existence of large amplitude limit cycles could be due to the particular system parameters used in Figure 17 since the author could not determine their existence in Figures 15 or 16. However, even if they were found to exist in these figures, they probably would not be found in a physical system for the reasons given above.

The response of the compensated control system to simple input signals can be analyzed using phase-plane trajectories in a manner similar to the approach used in

Chapter IV. From Figure 14, the equation for $E_3(z)$ can be written as

$$E_3(z) = R(z) + E_2(z). \tag{5-5}$$

Taking the inverse Z transform,

$$e_3(kT) = r(kT) + e_2(kT) \tag{5-6}$$

$$= r(kT) + Ky(kT) + x(kT) \tag{5-7}$$

and

$$\Delta e_3(kT) = \Delta r(kT) + K\Delta y(kT) + \Delta x(kT). \tag{5-8}$$

However, to retain the validity of the initial condition equations, i.e. equations 4-31 and 4-34, the coordinates x and y are used on the phase-planes. Therefore, the values read from the phase-plane trajectories are

$$e(kT) = r(kT) + y(kT) + x(kT) \tag{5-9}$$

where

$$e(kT) = r(kT) - c(kT). \tag{5-10}$$

If the scale Ky were also shown along the y axis, the value $e_3(kT)$ could be read directly.

The system response to the ramp input of equation 4-41 with slope A equal to -0.5 and r(0) equal to zero is shown in Figure 20 using various different initial conditions and gain, K, equal to two. The trajectories shown in this figure may be compared with those of Figure 11 to see the difference between the compensated and uncompensated system. Observable in Figure 20 is the fact that the stable limit cycle is not centered at the origin. The average value of the oscillation is equivalent to a system lag in following the input signal.

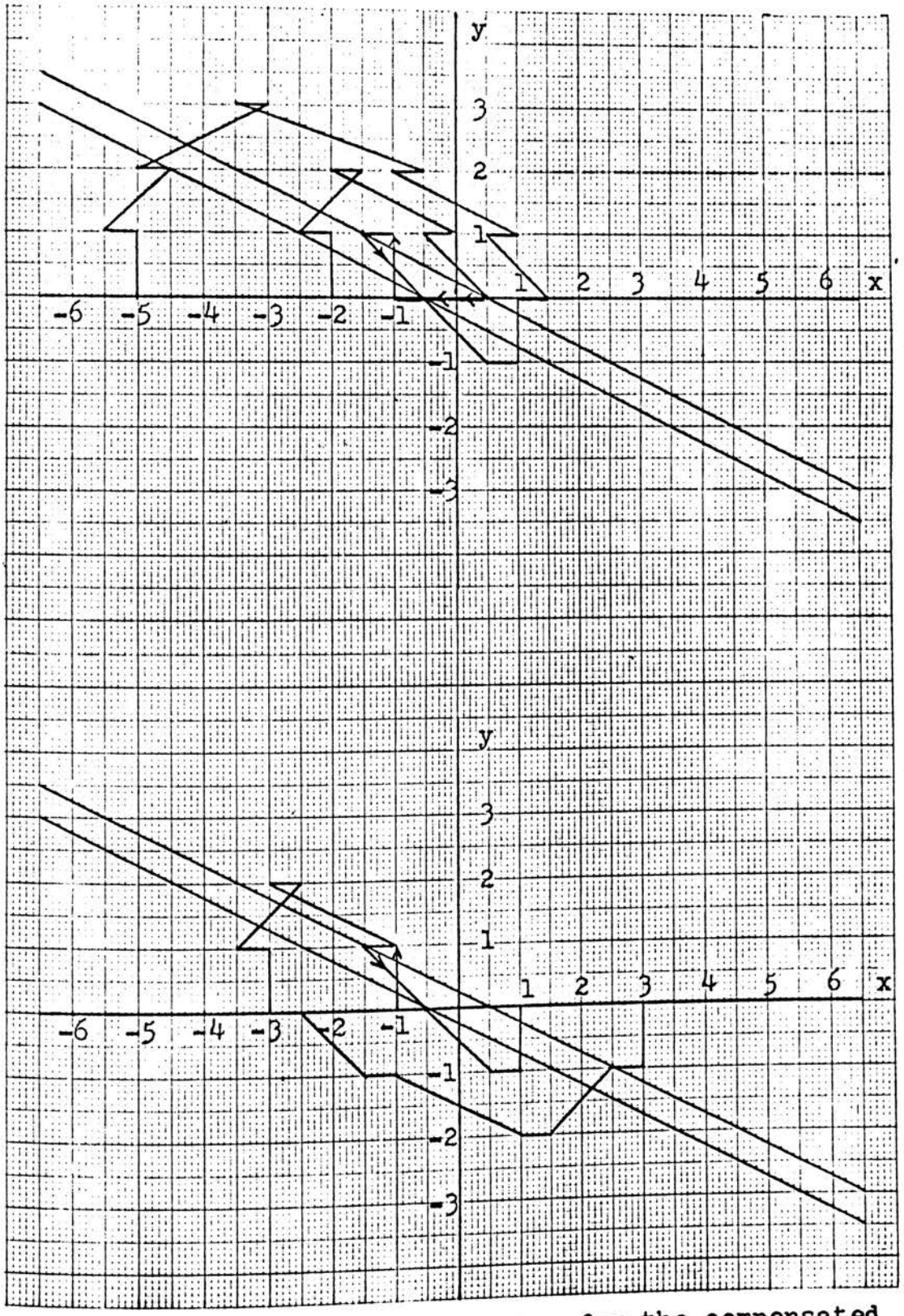

Figure 20. Phase-plane trajectories for the compensated system with K=2 and α=0.5 and a ramp input A=-.5.

At the beginning of this chapter a compensation element corresponding to the value of $K \neq 1$ was mentioned. The structure of this compensator is developed in the following paragraphs.

The block diagram of Figure 14 can be drawn in the equivalent form shown in Figure 21. It should be noted that for $K = 1$, the diagrams shown in Figures 3c and 21 are identical. Thus, the feedback signal $B(z)$ is a compensating signal.

The equation for the compensating signal can be written as

$$B(z) = (K-1)(1-z^{-1})\, C(z). \tag{5-11}$$

The inverse Z transform of this equation gives

$$b(kT) = (K-1)[c(kT) - c(kT-T)]. \tag{5-12}$$

Equation 5-12 describes the process by which the system has been compensated. It is apparent that the compensation signal $b(kT)$ is proportional to the rate of change in output position if the output position varies slowly in comparison to the sampling period. The constant of proportionality is

$$K_5 = (K-1)T \tag{5-13}$$

since the derivative of the output can be expressed approximately as

$$c'(kT) \approx \frac{c(kT) - c(kT-T)}{T} \tag{5-14}$$

From Figure 21, the compensated error signal when $R(z) = 0$. is given as

$$E_3(z) = -C(z) - B(z). \tag{5-15}$$

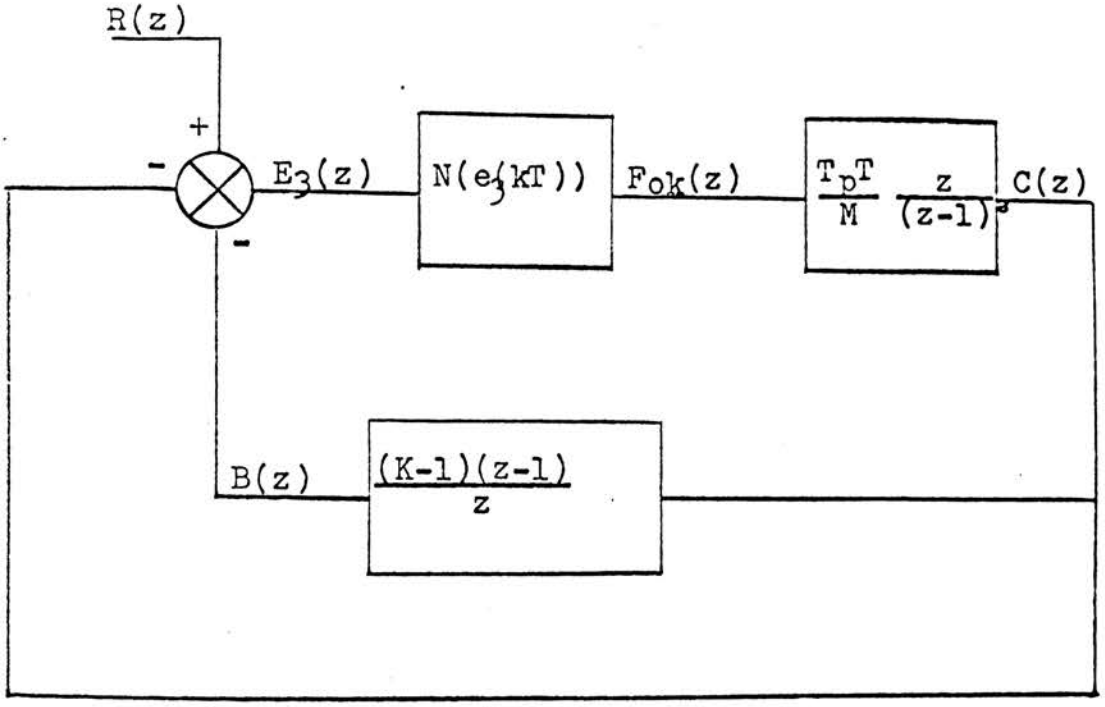

Figure 21. Feedback Compensation Block Diagram

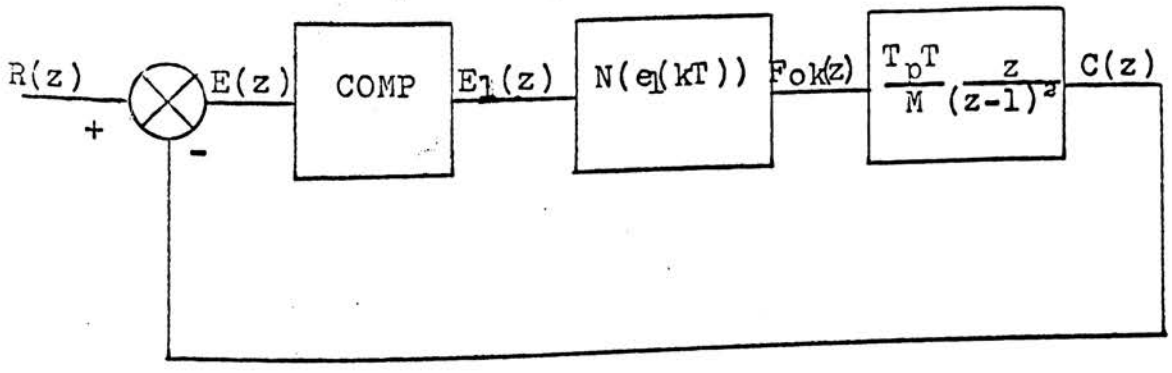

Figure 22. Cascade Compensation Block Diagram

The inverse transform yields

$$e_3(kT) = -c(kT) - b(kT). \tag{5-16}$$

Substituting equation 5-12 into 5-16, one gets

$$e_3(kT) = -c(kT) - (K-1)[c(kT) - c(kT-T)]. \tag{5-17}$$

The above equation shows that compensation is achieved through negative rate feedback. The equation also shows that positive rate feedback occurs if $K<1$. Since positive rate feedback corresponds to destabilization, only values of $K \geq 1$ are allowed.

In a practical system, the signal measured would probably be the position error given as

$$e(kT) = r(kT) - c(kT) \tag{5-18}$$

rather than the explicit value of output position. The compensator would then become a part of the forward path as shown in Figure 22. Equation 5-17 then becomes

$$e_1(kT) = e(kT) + (K-1)[e(kT) - e(kT-T)]. \tag{5-19}$$

The compensator described by equation 5-19 is easily implemented if the equation is rewritten as

$$e_1(kT) = Ke(kT) + (K-1)e(kT-T). \tag{5-20}$$

Figure 23 shows the corresponding block diagram. The series zero order hold circuits act as a shift register so that the value of $e(kT-T)$ is not destroyed at the next sampling, i.e. at time $t = kT$.

This chapter has presented a method of phase-plane analysis which can be used to determine the appropriate gain factors to use in a compensator of the form shown. The optimum gain values must be determined by the response

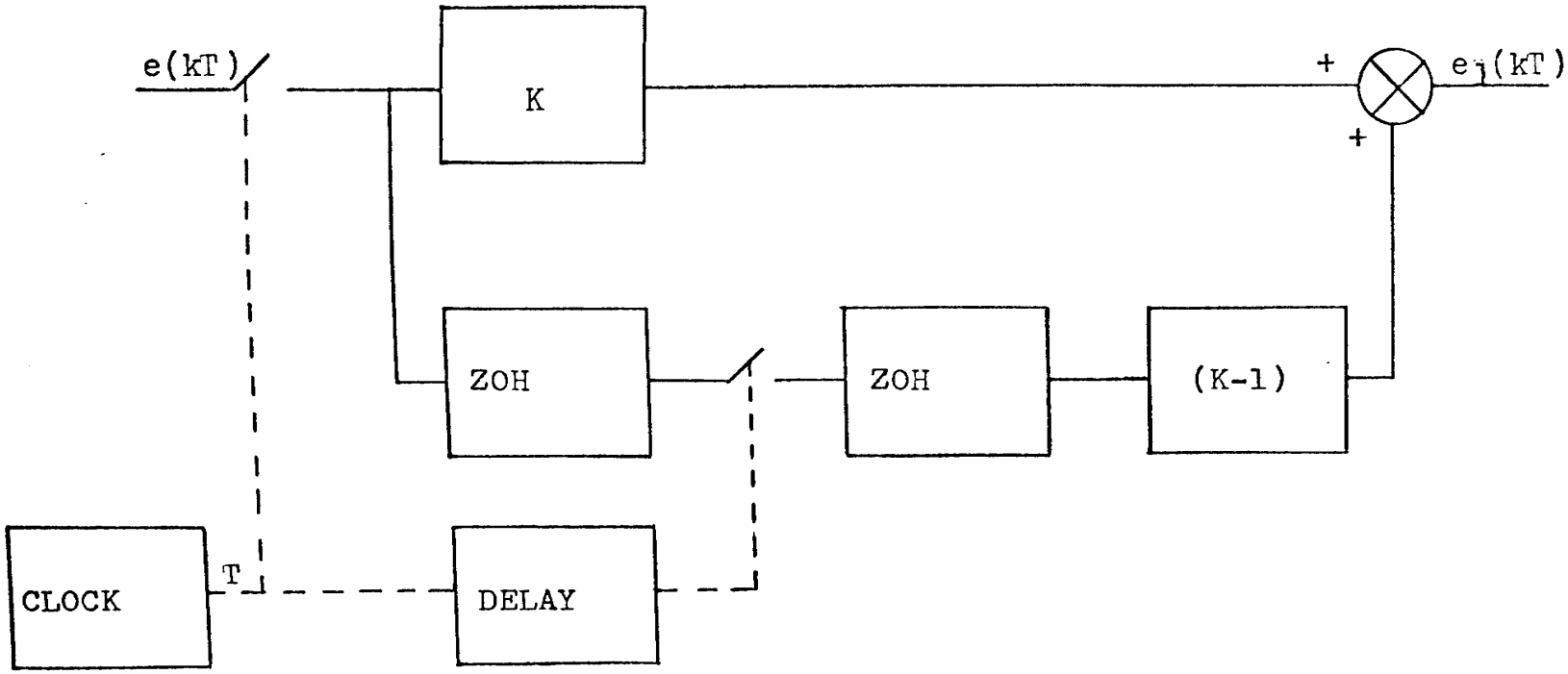

Figure 23. Compensation Network

desired from each particular control system.

The value of necessary gain is also closely associated with system parameters such as sampling period, control force amplitude, control force duration, vehicle mass, etc. Since the range of values of each of these parameters is limited by environmental conditions and other design criteria, these characteristics must be considered in the phase-plane construction.

Since it is not possible to consider the effects of external forces in phase-plane analysis, the system analysis would probably culminate in a digital or hybrid simulation to determine their effect.

CHAPTER VI

DIGITAL COMPUTER SIMULATION

The nonlinear sampled data control system under investigation can be simulated on a digital computer. This simulation can be used to determine the effect external forces have on the system.

The block diagrams of the compensated system which include the effects of the external force are shown in Figure 24. With the aid of these diagrams, the following equations can be written.

$$e(kT) = r(kT) - c(kT) \tag{6-1}$$

$$e_1(kT) = Ke(kT) + (K-1)e(kT-T) \tag{6-2}$$

$$f_{ok}(kT) = \begin{cases} F & , e_1(kT) \geq \alpha \\ 0 & , |e_1(kT)| < \alpha \\ -F & , e_1(kT) \leq -\alpha \end{cases} \tag{6-3}$$

These equations have been derived in previous chapters. Equation 6-3 is merely equation 4-16 with subscripts added to correspond to the compensated system.

The change in position (see Chapter III) during the period between samples is given as

$$\Delta c_{ok}(kT) = [K_f T/M] f_{ok}(kT). \tag{6-4}$$

By differentiating equation 3-8 and changing notation, the change in position rate is given as

$$\Delta c'_{ok}(kT) = [T_p/M] f_{ok}(kT). \tag{6-5}$$

Initial conditions are not included in either equations 6-4 or 6-5. However, these are accounted for later in the position and rate equations which correspond to external

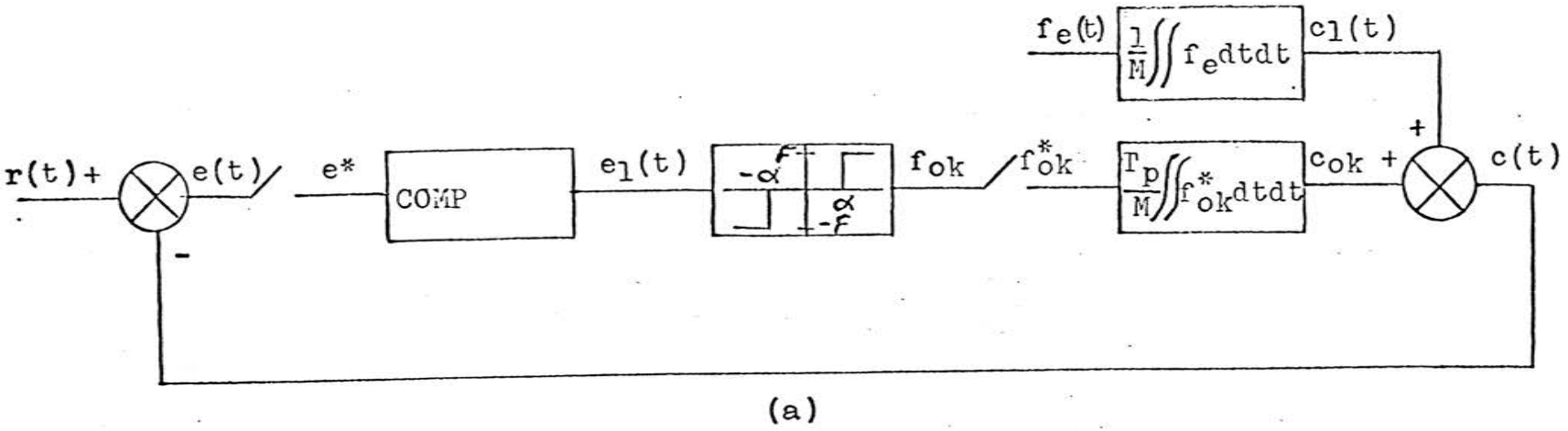

(a)

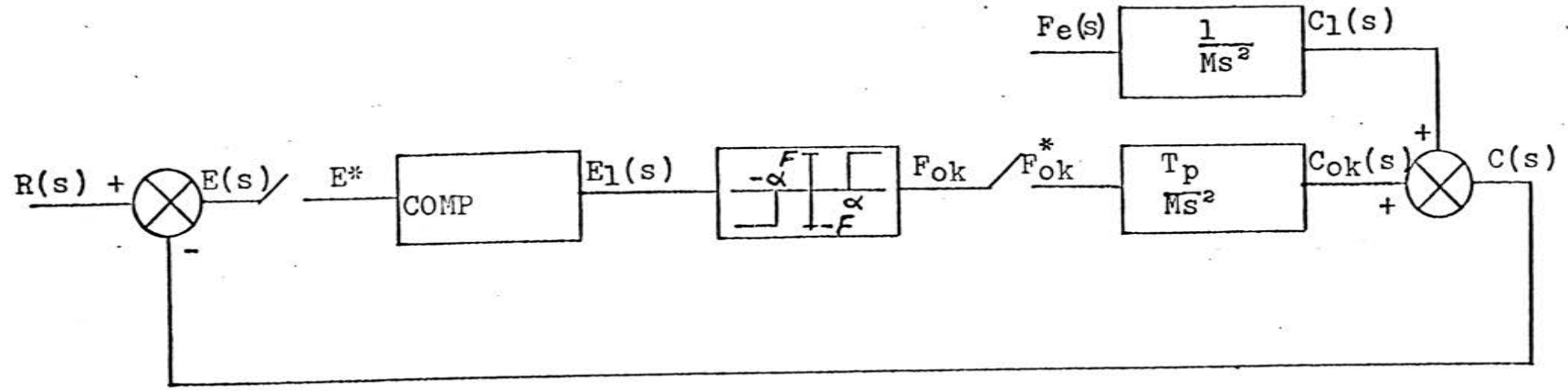

(b)

Figure 24 Compensated System Block Diagrams. a) Time Equations
b) Laplace Transformed Equations

force application.

For any external force, the position due to that force can be written as

$$c_1(kT+T) = \left[L^{-1}\left[\frac{F_e(s)}{Ms^2}\right]\right]_{t=kT}^{t=kT+T} + c_1(kT) + Tc_1'(kT) \quad (6\text{-}6)$$

and the rate as

$$c_1'(kT+T) = \left[L^{-1}\left[\frac{F_e(s)}{Ms}\right]\right]_{t=kT}^{t=kT+T} + c_1'(kT). \quad (6\text{-}7)$$

The total position is therefore given by

$$c(kT+T) = [K_fT/M]f_{ok}(kT) + \left[L^{-1}\left[\frac{F_e(s)}{Ms^2}\right]\right]_{kT}^{kT+T} + c(kT) + Tc'(kT), \quad (6\text{-}8)$$

where notation has been changed from that of equation 6-6 since it was stated earlier that all initial conditions would be accounted for in equations 6-6 and 6-7.

The total rate is given by

$$c'(kT+T) = [T_p/M]f_{ok}(kT) + \left[L^{-1}\left[\frac{F_e(s)}{Ms}\right]\right]_{kT}^{kT+T} + c'(kT). \quad (6\text{-}9)$$

The external force applied to a space vehicle would probably vary slowly. If the assumption is made that the external force is constant for a small number of sample periods, equations 6-8 and 6-9 can be written as

$$c(kT+T) = [K_fT/M]f_{ok}(kT) + .5F_1T^2/M + c(kT) + Tc'(kT) \quad (6\text{-}10)$$

and

$$c'(kT+T) = [T_p/M]f_{ok}(kT) + F_1T/M + c'(kT) \quad (6\text{-}11)$$

where F_1 is the magnitude of the external force.

The previously defined equations may be combined to form a digital computer simulation of the feedback control system. A program for this simulation is given in Appendix I. It should be noted that in this simulation a value of K=1 corresponds to the uncompensated system while values of $K \neq 1$ correspond to various amounts of compensation.

This program provides a means to study the response of the control system under the influence of external forces when a step and/or ramp input signal is applied.

Since the incremental phase-plane is an exact solution to the system equations, the computer was programmed using initial conditions corresponding to those used in the phase-plane analyses of Chapters IV and V. Identical results were obtained using the computer simulation.

In addition, the computer was programmed using two values of constant external force and several different compensator gains. Representative solutions are shown in the following graphs for various initial conditions.

Several interesting characteristics are observed in these solutions. As in the situation without external forces, large amplitude oscillations result for the forced system with the amplitude depending upon the initial conditions of the system.

In the compensated system, the small amplitude steady state limit cycle is seen to possess an average position error. The magnitude of this average error is dependent

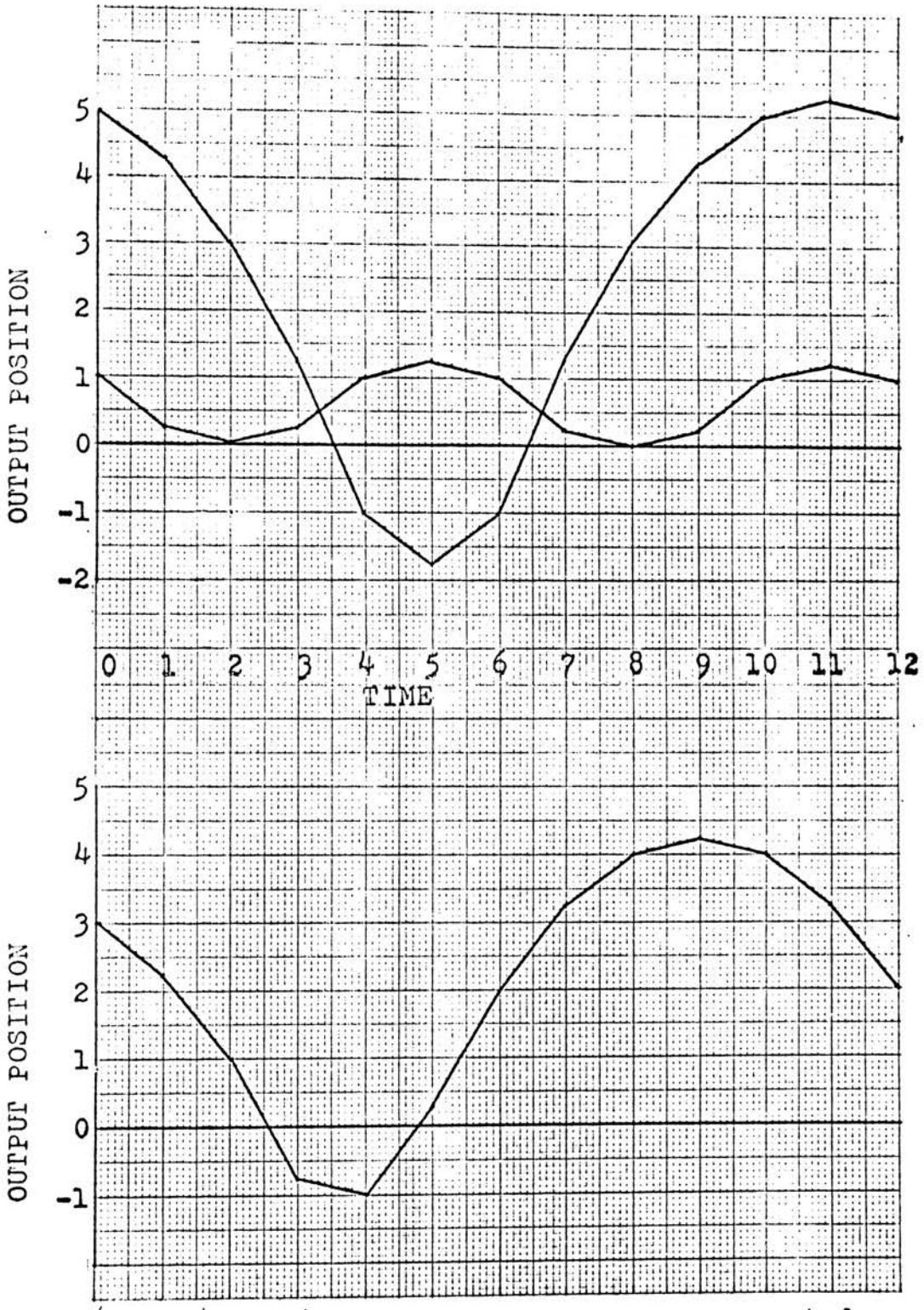

Figure 25. Output position values for the uncompensated system with α=0.5 and an external force to mass ratio of 0.5.

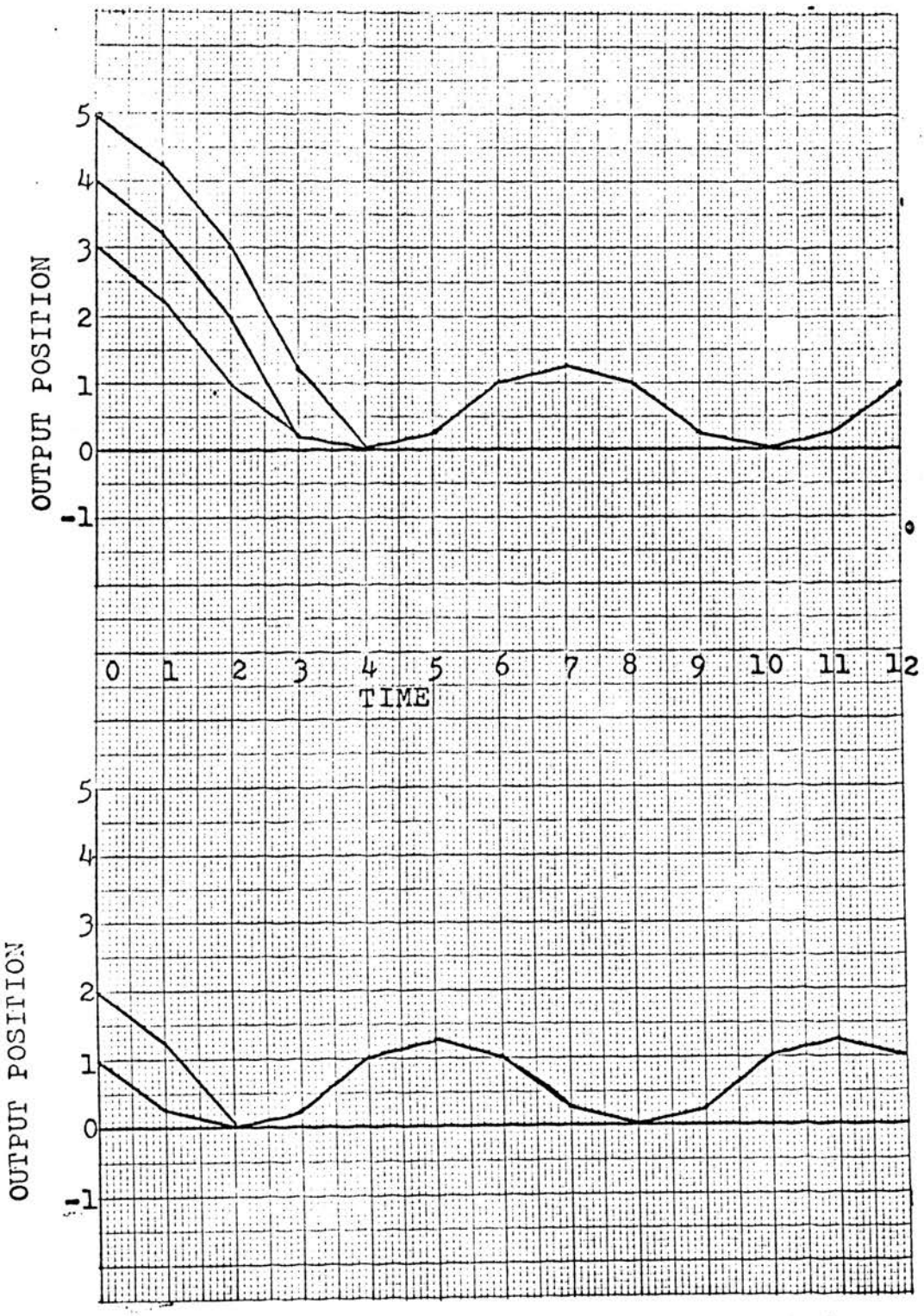

Figure 26. Output position values for the compensated system with K=1.5 and α=0.5 and an external force to mass ratio of 0.5.

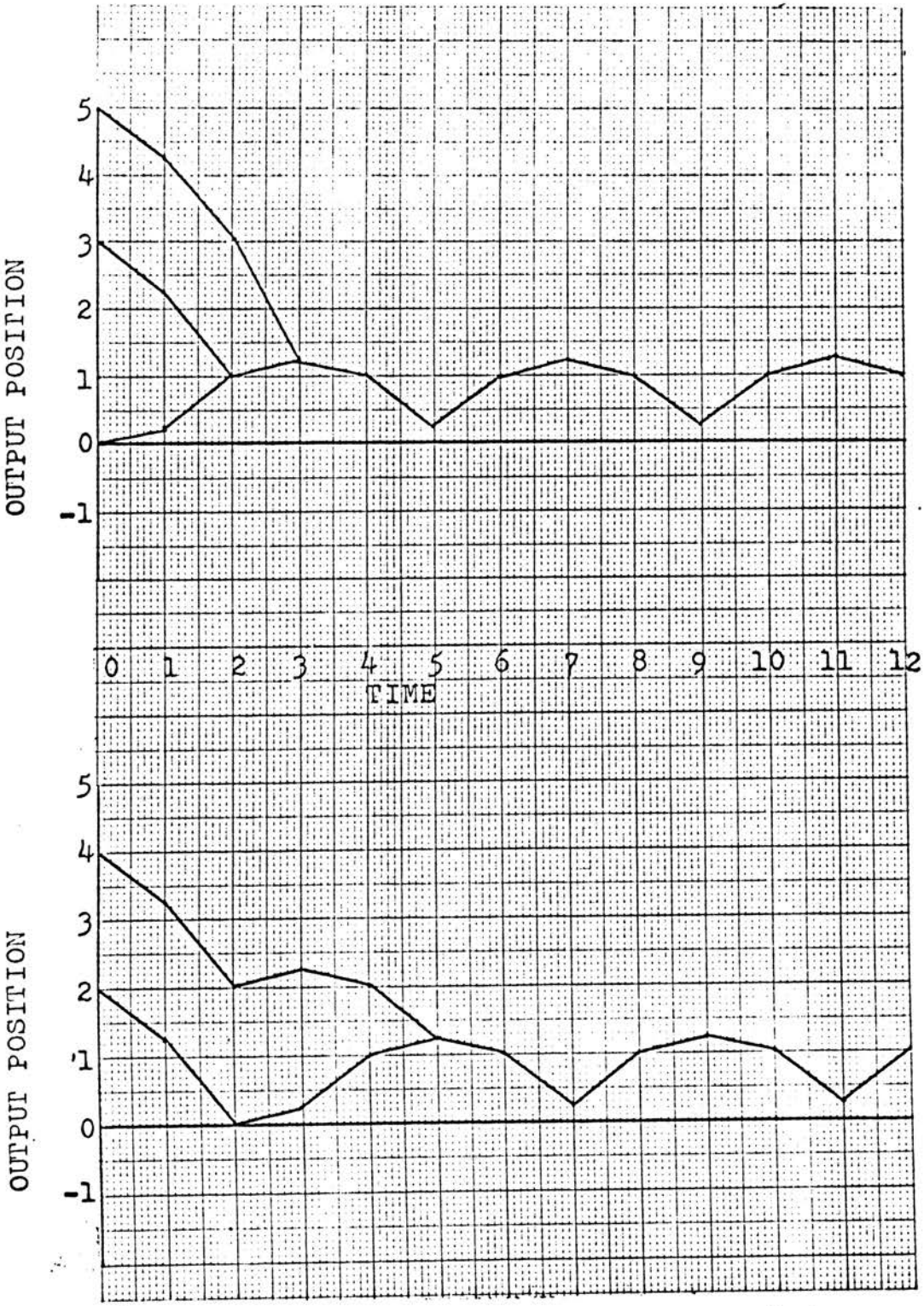

Figure 27. Output position values for the compensated system with K=3 and α=0.5 and an external force to mass ratio of 0.5.

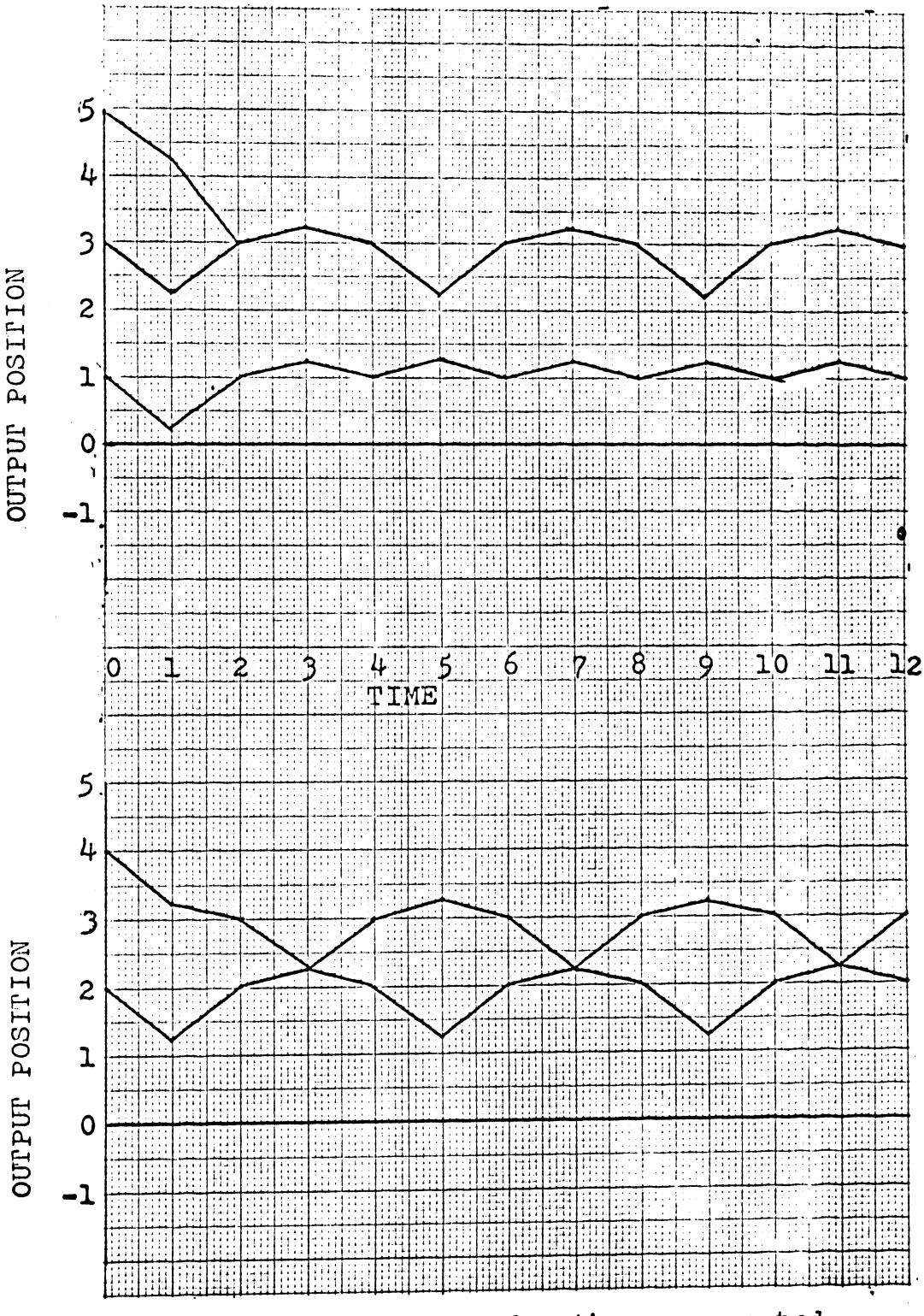

Figure 28. Output position values for the compensated system with K=5 and α=0.5 and an external force to mass ratio of 0.5.

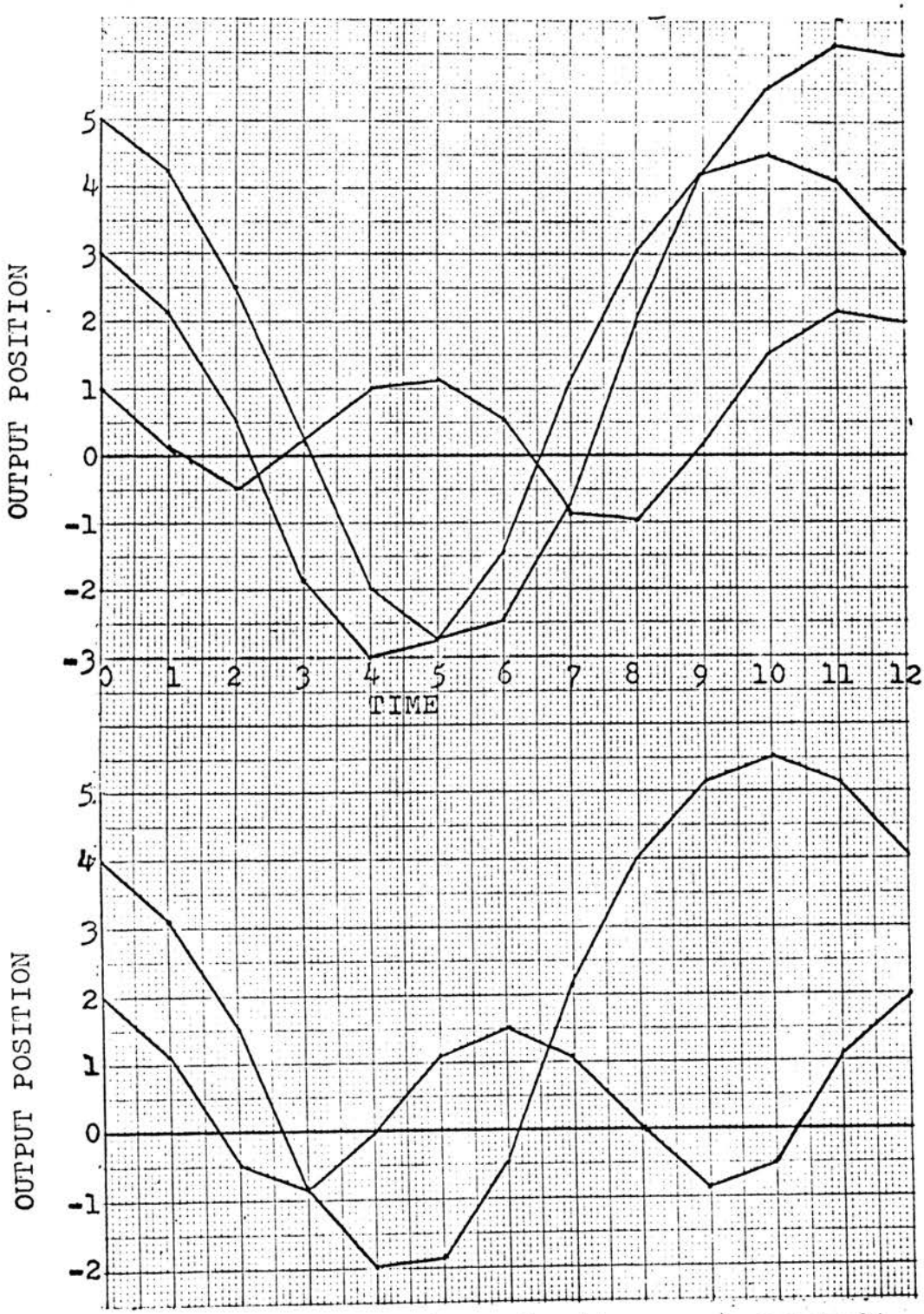

Figure 29. Output position values for the uncompensated system with $\alpha=0.5$ and an external force to mass ratio of 0.25.

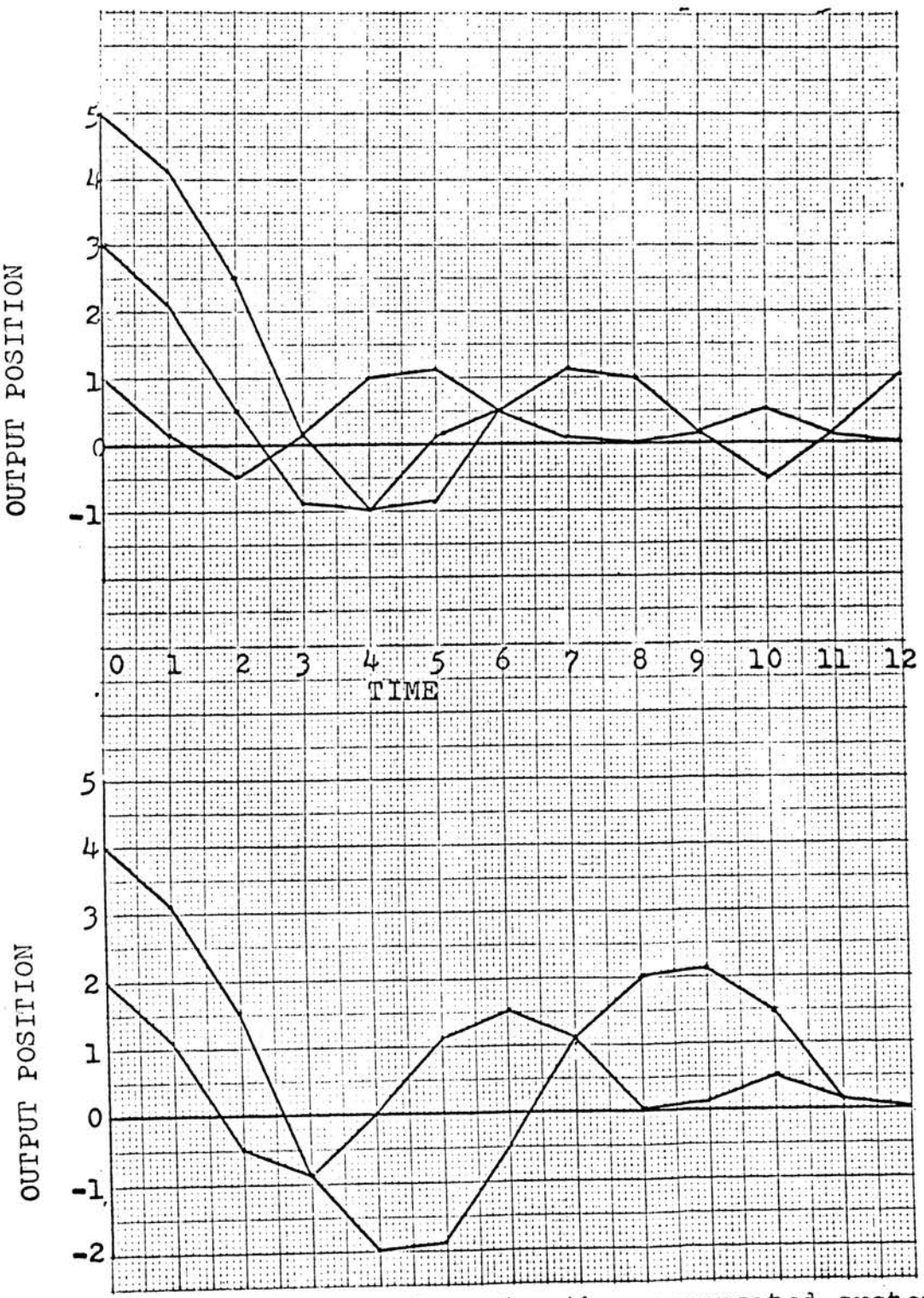

Figure 30. Output position values for the compensated system with K=1.5 and α=0.5 and an external force to mass ratio of 0.25.

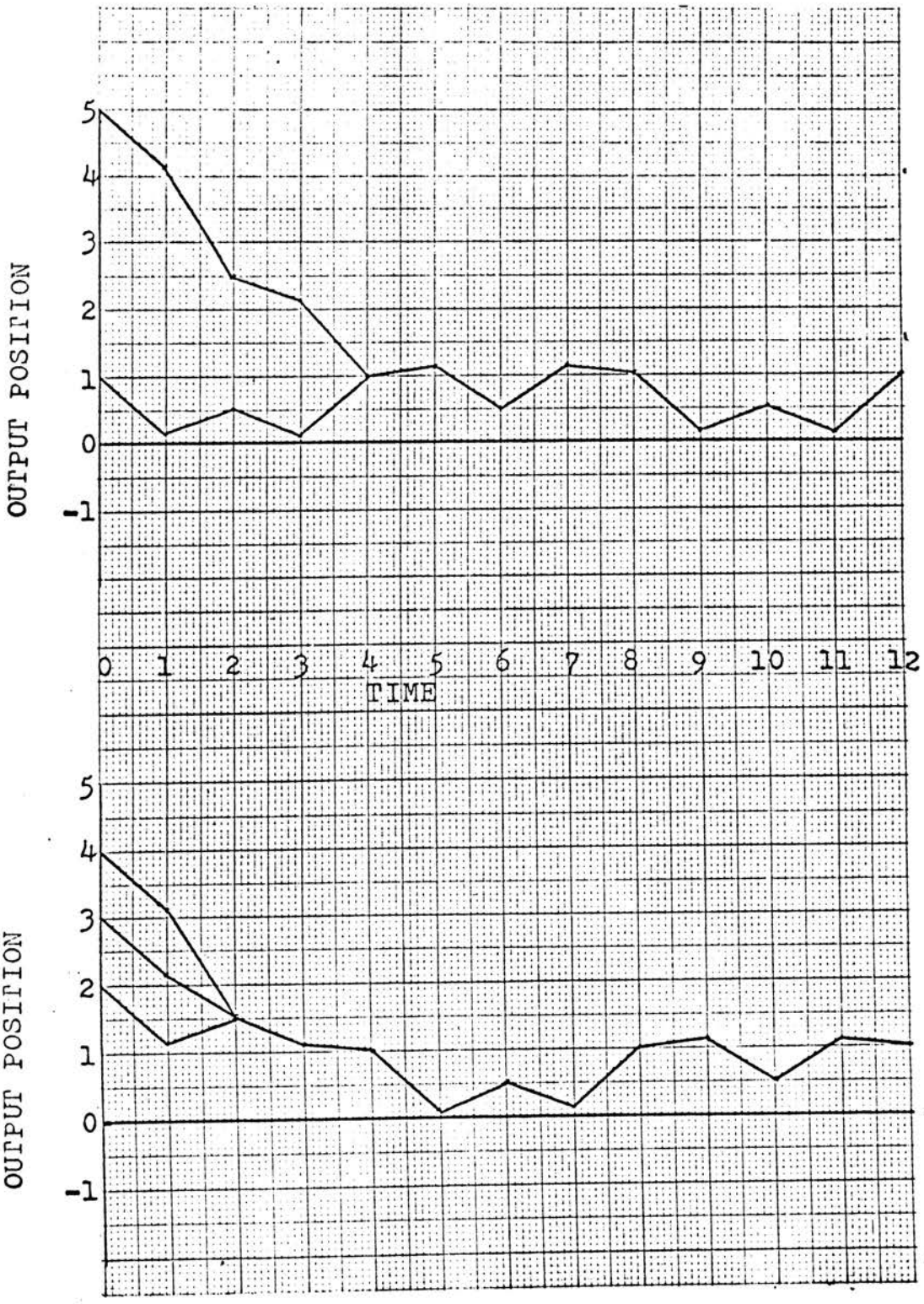

Figure 31. Output position values for the compensated system with K=3 and α=0.5 and an external force to mass ratio of 0.25.

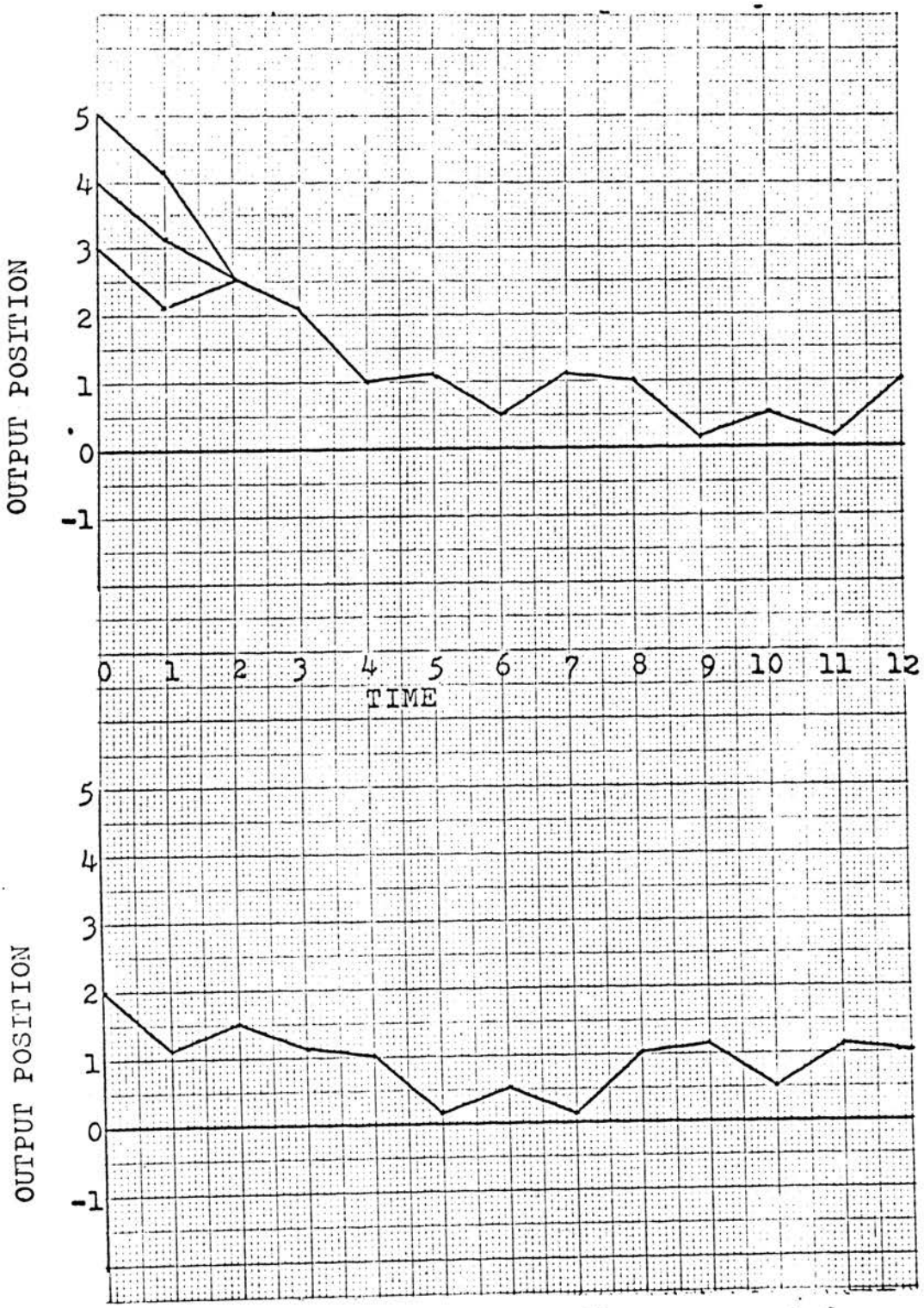

Figure 32. Output position values for the compensated system with K=5 and α=0.5 and an external force to mass ratio of 0.25.

upon the value of compensator gain. The graphs show that the average error is greater when large values of gain are used. These solutions indicate that to insure small average error a value of K greater than 1, but less than 3 should be used.

The computer solutions also show that the time before the steady-state output conditions are reached is smaller for large values of compensator gain. The same conclusion can be reached by studying the phase-plane trajectories derived earlier.

The main conclusion that can be drawn from the position solutions obtained from the simulation is that satisfactory system response can be obtained when the vehicle is under the influence of external force fields. The optimum value of compensator gain must be determined for each individual set of vehicle parameters and environmental characteristics.

CHAPTER VII

CONCLUSIONS

The response characteristics of a nonlinear sampled data position control system employing pulsed thrust control have been analyzed using two basic techniques. The methods utilized were incremental phase-plane trajectory construction and digital computer system simulation.

Many conclusions concerning the system's stability and response characteristics have been reached in the previous chapters. The phase-plane analysis showed that the uncompensated system is stable in the sense that its output is not divergent. However, its response is oscillatory with the amplitude depending upon initial conditions. Its output will follow a ramp or slowly varying input signal, but the oscillations will be superimposed upon this response.

The phase-plane analysis, utilizing a change in variables, aided in the design of a compensator and provided the analysis of the compensated system. The output of this system was seen to converge to a small amplitude, steady state, limit cycle response. The amplitude of this limit cycle is closely governed by the dead zone limits of the system. This system gives a satisfactory response for step, ramp, and slowly varying input signals.

The response for the system when under the influence of external forces proved to be adequate provided the control force was sufficient to overcome the impressed acceleration.

The application of external forces does cause an average position error to be present.

This thesis does not attempt to provide criteria for choosing optimum sampling periods, control force amplitudes, or control force durations. These, as well as the problems associated with designing for minimal fuel consumption, are closely associated with actual vehicle parameters and environmental characteristics and must be considered during actual vehicle design.

The investigation has shown that reaction jet pulses, each of constant amplitude and time duration, in conjunction with sampled data error information can provide satisfactory position and/or attitude control for a space vehicle.

APPENDIX I

DIGITAL COMPUTER PROGRAM

The digital computer program simulating the position control system is listed in this appendix.

This simulation allows the study of the control system response for the vehicle in a constant external force field. The program allows the external force to be of any magnitude, including zero.

Any combination of step and ramp input signals may be studied with this program. With slight modification, the response to sinusoidal input signals could also be studied.

The definition of the program variables is given in the following list.

$R(K) = f(kT-T)$	input signal
$CT(K) = c(kT-T)$	output position
$CTP(K) = c'(kT-T)$	output position rate
$E(K) = e(kT-T)$	error signal
$E1(K) = e_1(kT-T)$	compensated error signal
$FO(K) = f_{ok}(kT-T)$	control force
$ALPHA = \alpha$	dead zone limit
$BETA = A$	slope of ramp input
$GAINK = K$	compensator gain
$TP = T_p$	control force duration
$T = T$	sampling period
$TPOT = T_p/T$	time ratio

WTMAS = M	Mass
Fl = F_1	magnitude of constant external force
F = F	magnitude of control force

```
      A NONLINEAR SAMPLED DATA POSITION CONTROL SYSTEM SIMULATION
      CONTROL SYSTEM EMPLOYS PULSED THRUST CONTROL
      DIMENSION R(100),CT(100),CTP(100),E(100),FO(100),E1(100)
      READ 200,I,L
      READ 400,TP,TPOT,WTMAS,T,F1,F
      DO 500 J=1,L
      READ 400,ALPHA,R(1),CT(1),CTP(1),BETA,GAINK
    1 TPOM=TP/WTMAS
    2 TMHTP=T*(1.-TPOT/2.)
    3 TPMT=TPOM*TMHTP
    4 FTT2M=F1*T*T/(2.*WTMAS)
    5 FTOM=F1*T/WTMAS
      N=I+1
   71 E(1)=R(1)-CT(1)
      E1(1)=GAINK*E(1)
   72 IF(E1(1)-ALPHA)73,74,74
   73 IF(E1(1)+ALPHA)75,75,76
   74 FO(1)=F
      GO TO 77
   75 FO(1)=-F
      GO TO 77
   76 FO(1)=0.0
   77 CT( 2 )=FO(1)*TPMT+FTT2M+CT(1)+T*CTP(1)
   78 CTP(2  )=FO(1)*TPOM+FTOM+CTP(1)
   79 R(2)=BETA*T+R(1)
   10 DO 19 K=2,I
   11 E(K)=R(K)-CT(K)
      E1(K)=GAINK*E(K)-(GAINK-1.0)*E(K-1)
   12 IF(E1(K)-ALPHA)13,14,14
   13 IF(E1(K)+ALPHA)15,15,16
   14 FO(K)=F
      GO TO 17
   15 FO(K)=-F
      GO TO 17
   16 FO(K)=0.0
   17 CT(K+1)=FO(K)*TPMT+FTT2M+CT(K)+T*CTP(K)
   18 CTP(K+1)=FO(K)*TPOM+FTOM+CTP(K)
   19 R(K+1)=BETA*T+R(K)
   25 E(N)=R(N)-CT(N)
   26 E1(N)=GAINK*E(N)-(GAINK-1.0)*E(I)
   55 PRINT 305
   60 PRINT 120,(K,E(K),R(K),CT(K),CTP(K),E1(K),K=1,N)
  500 PRINT 550,TP,TPOT,WTMAS,T,F1,F,ALPHA,BETA,GAINK
  120 FORMAT (I12,5F12.5)
  200 FORMAT(2I5)
  305 FORMAT(16X,4HE(K),8X,4HR(K),7X,5HCT(K),7X,6HCTP(K),6X,5HE1(K))
  400 FORMAT (6E12.5)
  550 FORMAT (9F8.4)
      PARAMETERS LISTED ARE TP,TPOT,WTMAS,T,F1,F,ALPHA,BETA,GAINK
      CALL EXIT
      END
```

BIBLIOGRAPHY

1. Pistiner, J. S. "On-Off Control System for Attitude Stabilization of a Space Vehicle." ARS Journal, Vol. 29: April, 1959, pp 283-289.

2. Marx, M. F. "Design Aspects of Attitude Control Systems." IRE Transactions, AC-6: February, 1961, pp 67-73.

3. Dahl, P. R., Aldrich, G. T., and Herman, L. K. "Limit Cycles in Reaction Jet Attitude Control Systems." Progress in Astronautics and Rocketry - Vol. 8. Academic Press, New York: 1962, pp 599-628.

4. Gaylord, R. S. and Keller, W. N. "Attitude Control System Using Logically Controlled Pulses." Progress in Astronautics and Rocketry - Vol. 8. Academic Press, New York: 1962, pp 629-648.

5. Vaeth, J. E. "Vapor Jet Control of Space Vehicles." IRE Transactions, AC-7: October, 1962, pp 67-74.

6. Vaeth, J. E. "Compatibility of Impulse Modulation Techniques with Attitude Sensor Noise and Spacecraft Maneuvering." IEEE Transactions, AC-10: January, 1965, pp 67-76.

7. Ragazzini, J. R. and Franklin, G. F. Sampled-Data Control Systems. McGraw-Hill Book Co., Inc., New York: 1958.

8. Lindorff, D. P. Theory of Sampled-Data Control Systems. John Wiley & Sons, Inc., New York: 1965.

9. DeRusso, P. M. Roy, R. J. and Close, C. M. State Variables for Engineers. John Wiley & Sons, Inc., New York: 1965.

10. Truxal, J. G. Automatic Feedback Control System Synthesis. McGraw-Hill Book Co., Inc., New York: 1955.

11. Aseltine, J. A. and Nesbit, R. A. "The Incremental Phase-Plane for Non-Linear Sampled Data Systems." IRE Transactions, AC-5: August, 1960, pp 159-165.

12. Lindorff, D. P. "Use of a Coordinate Transformation in the Incremental Phase Plane." IEEE Transactions, AC-9: January, 1964, pp 110-113.

13. Jury, E. I. Theory and Application of the Z-Transform Method. John Wiley & Sons, Inc., New York: 1964.

14. D'Azzo, J. J. and Houpis, C. H. Feedback Control System Analysis and Synthesis. McGraw-Hill Book, Inc., New York: 1960.

15. Kuo, B. C. Analysis and Synthesis of Sampled-Data Control Systems. Prentice-Hall, Inc., Englewood Cliffs, N. J. : 1963.

16. Cosgriff, R. L. Nonlinear Control Systems. McGraw-Hill Book Company, Inc., New York: 1958.

VITA

The author was born on March 5, 1942, in St. Charles, Missouri where he also received his primary and secondary education.

In September, 1960, he entered the University of Missouri, School of Mines and Metallurgy. During his undergraduate career, he supplemented his education with engineering experience as a Co-op Student with McDonnell Aircraft Corporation, St. Louis, Missouri. He received a Bachelor of Science Degree in Electrical Engineering from the University of Missouri at Rolla in May, 1965.

He has been enrolled in Graduate School of the University of Missouri at Rolla since September, 1965, and has held a National Defense Education Act, Title IV, Fellowship for the period September, 1965, to June, 1966.

He is a member of IEEE, Phi Kappa Phi, Tau Beta Pi, and Eta Kappa Nu.